

Jouni Pakarinen

RECOVERY AND REFINING OF MANGANESE AS BY-PRODUCT FROM HYDROMETALLURGICAL PROCESSES

Thesis for the degree of Doctor of Science (Technology) to be presented with due permission for public examination and criticism in the Auditorium of the Student Union House at Lappeenranta University of Technology, Lappeenranta, Finland on 28th of October 2011, at noon.

Acta Universitatis
Lappeenrantaensis 442

Supervisor	Prof. Erkki Paatero Laboratory of Industrial Chemistry Department of Chemical Technology Faculty of Technology Lappeenranta University of Technology Lappeenranta, Finland
Reviewers	Associate Prof. Don Ibana Metallurgical and Minerals Engineering Curtin University Perth, Australia
	Dr. Gabor Csicsovski Buchan Department of Mining Queen's University Kingston, Canada
Opponent	Dr. Gabor Csicsovski Buchan Department of Mining Queen's University Kingston, Canada

ISBN 978-952-265-135-8
ISBN 978-952-265-136-5 (PDF)
ISSN 1456-4491

Lappeenrannan teknillinen yliopisto
Digipaino 2011

ABSTRACT

Jouni Pakarinen

Recovery and refining of manganese as by-product from hydrometallurgical processes

Lappeenranta, 2011

64 p.

Acta Universitatis Lappeenrantaensis 442

Diss. Lappeenranta University of Technology

ISBN 978-952-265-136-5 (PDF), ISBN, 978-952-265-135-8, ISSN 1456-4491

The consumption of manganese is increasing, but huge amounts of manganese still end up in waste in hydrometallurgical processes. The recovery of manganese from multi-metal solutions at low concentrations may not be economical. In addition, poor iron control typically prevents the production of high purity manganese. Separation of iron from manganese can be done with chemical precipitation or solvent extraction methods. Combined carbonate precipitation with air oxidation is a feasible method to separate iron and manganese due to the fast kinetics, good controllability and economical reagents. In addition the leaching of manganese carbonate is easier and less acid consuming than that of hydroxide or sulfide precipitates. Selective iron removal with great efficiency from MnSO_4 solution is achieved by combined oxygen or air oxidation and CaCO_3 precipitation at $\text{pH} > 5.8$ and at a redox potential of > 200 mV. In order to avoid gypsum formation, soda ash should be used instead of limestone. In such case, however, extra attention needs to be paid on the reagents mole ratios in order to avoid manganese co-precipitation.

After iron removal, pure MnSO_4 solution was obtained by solvent extraction using organophosphorus reagents, di-(2-ethylhexyl)phosphoric acid (D2EHPA) and bis(2,4,4-trimethylpentyl)phosphinic acid (CYANEX 272). The Mn/Ca and Mn/Mg selectivities can be increased by decreasing the temperature from the commonly used temperatures ($40 - 60^\circ\text{C}$) to 5°C . The extraction order of D2EHPA (Ca before Mn) at low temperature remains unchanged but the lowering of temperature causes an increase in viscosity and slower phase separation. Of these reagents, CYANEX 272 is selective for Mn over Ca and, therefore, it would be the better choice if there is Ca present in solution. A three-stage Mn extraction followed by a two-stage scrubbing and two-stage sulfuric acid stripping is an effective method of producing a very pure MnSO_4 intermediate solution for further processing.

From the intermediate MnSO_4 some special Mn- products for ion exchange applications were synthesized and studied. Three types of octahedrally coordinated manganese oxide materials as an alternative final product for manganese were chosen for synthesis: layer structured Nabirnessite, tunnel structured Mg-todorokite and K-kryptomelane. As an alternative source of pure MnSO_4 intermediate, kryptomelane was synthesized by using a synthetic hydrometallurgical tailings. The results show that the studied OMS materials adsorb selectively Cu, Ni, Cd and K in the presence of Ca and Mg. It was also found that the exchange rates were reasonably high due to the small particle dimensions. Materials are stable in the studied conditions and their maximum Cu uptake capacity was 1.3 mmol/g. Competitive uptake of metals and acid was studied using equilibrium, batch kinetic and fixed-bed measurements. The experimental data was correlated with a dynamic model, which also accounts for the dissolution of the framework manganese.

Manganese oxide micro-crystals were also bound onto silica to prepare a composite material having a particle size large enough to be used in column separation experiments. The MnOx/SiO₂ ratio was found to affect significantly the properties of the composite. The higher the ratio, the lower is the specific surface area, the pore volume and the pore size. On the other hand, higher amount of silica binder gives composites better mechanical properties. Birnesite and todorokite can be aggregated successfully with colloidal silica at pH 4 and with MnO₂/SiO₂ weight ratio of 0.7. The best gelation and drying temperature was 110°C and sufficiently strong composites were obtained by additional heat-treatment at 250°C for 2 h. The results show that silica-supported MnO₂ materials can be utilized to separate copper from nickel and cadmium. The behavior of the composites can be explained reasonably well with the presented model and the parameters estimated from the data of the unsupported oxides. The metal uptake capacities of the prepared materials were quite small. For example, the final copper loading was 0.14 mmol/g_{MnO₂}. According to the results the special MnO₂ materials are potential for a specific environmental application to uptake harmful metal ions.

Keywords: Manganese, Iron, Tailings, Precipitation, Solvent Extraction, Ion Exchange, Molecular Sieve, Hydrometallurgy

UDC 669.053.4:669.74:622.75/.77

TIIVISTELMÄ

Jouni Pakarinen

Mangaanin talteenotto ja jalostus hydrometallurgisen prosessin sivutuotteena

Lappeenranta, 2011

64 s.

Acta Universitatis Lappeenrantaensis 442

Diss. Lappeenranta University of Technology

ISBN 978-952-265-136-5 (PDF), ISBN, 978-952-265-135-8, ISSN 1456-4491

Mangaanin kulutus on lisääntynyt tasaisesti, mutta siitä huolimatta hydrometallurgian prosesseissa suuri määrä mangaania päätyy jätteeksi, sillä hyödyntäminen laimeista monimetalliliuoksista ei aina ole taloudellista. Myös huono raudan hallinta estää puhtaan mangaanin tuotannon. Rauta ja mangaani voidaan erottaa hydrometallurgisista liuoksista käyttäen kemiallista saostusta tai neste-nesteuuttoa. Yhdistetty karbonaattisaostus ja ilmahapetus on kuitenkin taloudellisesti ja teknisesti ehkä kaikkein järkevin menetelmä raudan ja mangaanin erottamisessa johtuen nopeasta kinetiikasta, prosessin hyvästä hallittavuudesta ja halvoista reagensseista. Lisäksi karbonaattirikasteen liuotus kuluttaa vähemmän happoa kuin esimerkiksi hydroksidi- tai sulfidirikasteen liuotus. Rauta saostuu selektiivisesti ja tehokkaasti $MnSO_4$ -liuoksesta kun käytetään yhdistettyä kalkkikivi ($CaCO_3$) -saostusta ja happi tai ilmahapetusta, ja kun liuos-pH > 5,8 ja hapetuspotentiaali > 200 mV. Mikäli halutaan välttää kipsin muodostuminen, on käytettävä soodaa (Na_2CO_3) kalkkikiven sijaan. Tässä tapauksessa on kuitenkin kiinnitettävä huomiota reagenssien moolisuhteisiin ja liuos-pH:n arvoon, jotta vältetään mangaanin myötäsaostuminen.

Raudan poiston ja konsentroinnin jälkeen puhdasta mangaanisulfaattiliuosta voidaan tuottaa käyttäen esimerkiksi di-(2-etyyliheksyyli)fosforihappo (D2EHPA) and bis(2,4,4-trimetyylipentyyli)fosfiinihappo (CYANEX 272) -reagensseja. Mn/Ca ja Mn/Mg -selektiivisyyksiä voidaan parantaa alentamalla lämpötilaa tyypillisesti käytetystä (40 – 60°C) 5°C:een. D2EHPA:n uuttautumisympäristö (Ca ennen Mn:a) pysyy kuitenkin samana ja lämpötilan alentaminen nostaa liuoksen viskositeettia, mikä heikentää faasien erottumista. CYANEX 272 on näistä reagensseista selektiivisempi Mn:lle Ca:n suhteen ja on siksi parempi vaihtoehto, jos liuoksessa on kalsiumia. Jatkuvatoinisella prosessilla, jossa on kolmiaskelinen lataus- sekä kaksiaskelinen pesu- ja takaisinuuvoavaihe (strippaus), saadaan tuotettua hyvin puhdasta $MnSO_4$ -välituotetta.

Puhdasta $MnSO_4$ -liuosta käytettiin lähtöaineena, kun syntetisoitiin ja tutkittiin Mn-tuotteita ioninvaihtosovelluksissa. Kolme erilaista oktaedrisesti koordinoitunutta mangaanioksidimateriaalia valittiin lopputuotteeksi: tasorakenteinen Na-birnesiitti ja tunnelirakenteiset Mg-todorokiitti sekä K-kryptomelaani. Lähtöliuoksena käytettiin sekä hydrometallurgista malliliuosta että puhdasta $MnSO_4$ -liuosta. Tulokset osoittavat, että syntetisoidut materiaalit adsorboivat selektiivisesti Cu:a, Ni:a, Cd:a ja K:a myös Ca:a ja Mg:a sisältävistä vesiliuoksista. Johtuen pienestä partikkelikoosta, aineensiirtonopeudet olivat riittävän suuria. Materiaalien havaittiin olevan stabiileja tutkituissa olosuhteissa, joissa suurimmaksi adsorptiokapasiteetiksi kuparille mitattiin 1,3 mmol/g. Kilpailevaa metallien ja

hapon adsorptiota tutkittiin sekä tasapaino-, panoskinetiikka- että kolonnikokeilla. Kokeellista dataa mallinnettiin dynaamisella mallilla, jossa myös mangaanin disproportio huomioitiin.

Kolonnikokeita varten oli mikrokokoisista mangaanioksidikiteistä valmistettava suurempia silikakomposiittipartikkeleita. MnO_x/SiO_2 -suhteen havaittiin vaikuttavan oleellisesti komposiitin ominaisuuksiin. Mitä suurempi suhde on, sitä pienempi on materiaalin ominaispinta-ala, huokostilavuus ja huokoskoko. Toisaalta silikan määrän lisääminen lisää komposiitin mekaanista lujuutta. Birnesiitti ja todorokiitti voidaan syntetisoida kolloidiseen silikaan pH:ssa 4 ja MnO_2/SiO_2 -painosuhteessa 0,7. Paras gelatointi- ja kuivauslämpötila oli 110°C. Lisäksi komposiiteista saatiin vielä vahvempia käsittelemällä niitä vielä 250°C:ssa 2 tuntia. Tulokset osoittavat, että silikasidottuja MnO_2 -materiaaleja voidaan hyödyntää kuparin erotuksessa nikkelistä ja kadmiumista. Komposiittien käyttäytyminen voidaan selittää riittävän hyvin esitellyllä mallilla ja käytetyillä parametreilla. Komposiittien metalliadsorptiokapasiteetit ovat aika pienet. Esimerkiksi kuparin latauskapasiteetti oli 14 mmol/g_{MnO2}. Tulosten perusteella MnO_2 -materiaalit ovat potentiaalisia raskasmetalliepäpuhtauksien talteenotossa ympäristösovelluksissa.

Avainsanat: Mangaani, Rauta, Sivuvirta, Saostus, Neste-nesteutto, Ioninvaihto, Molekyyliseula, Hydrometallurgia

UDC 669.053.4:669.74:622.75/.77

FOREWORD

It has been a pleasure to carry out this doctoral thesis in the Laboratory of Industrial Chemistry at Lappeenranta University of Technology during 2006 - 2011. I feel lucky to have the opportunity to enlighten me in this fascinating world of science. I wish to express my gratitude to my supervisor Prof. Erkki Paatero, for this great possibility, his belief in me and for his support during these years. I also thank him for challenging me to observe things from different view angles. Lic. tech. Markku Laatikainen deserves also special thanks for his valuable advices, comments and co-operation. Without his contribution this dissertation may not have become a reality.

The starting shoot of this dissertation was in 2005, when the manganese recovery subproject with OMG Finland Oy begun. Since that project, co-operation concerning manganese continued with Talvivaara Oyj. The projects were partly funded by the National Technology Agency (tekes). Mr. Kauko Karpale, Mr. Joni Hautojärvi, Ms. Marja Riekkola-Vanhanen and Mr. Leif Rosenback from co-operating companies deserve my warmest thanks. The financial support from the Academy of Finland is also gratefully acknowledged.

I am highly grateful to Ms. Anne Hyrkkänen and Ms. Krista Pussinen for assistance with the experimental and analytical work. I want to thank Dr. Kimmo Klemola for arranging the funding of the last year, and in addition, Mr. Markku Levomäki for solving several technical problems and for taking care of practical issues. Dr. Tuomo Sainio deserves many thanks for valuable advices and support. I want to give specially thank to Mr. Jussi Tamminen for interesting discussions and advises in the field of solvent extraction. In addition, I wish to express a special mention and thanks to the whole personnel of the Laboratory of Industrial Chemistry for the cheerful atmosphere.

I am grateful to my friends for giving me a counterbalance for the challenging work. Especially I want to thank my parents and Sisko and Osmo Jutila for supporting during these years. My wife Maarit deserves warm thanks for walking by my side and putting my feet on the ground. Finally, I wish to express the greatest gratitude to my wonderful son Joonatan for being in my life. This thesis is nothing compared to you.

Lappeenranta, 2011

Jouni Pakarinen

TABLE OF CONTENTS

1	INTRODUCTION.....	15
1.1	History and use of manganese	15
1.2	Occurrence and mining of manganese ores.....	17
1.3	Uptake and processing of manganese	17
1.3.1	Pyrometallurgy	17
1.3.2	Hydrometallurgy.....	18
1.4	Scope of the thesis.....	27
1.4.1	Objectives of the study.....	28
1.4.2	New findings	28
2.	EXPERIMENTAL	29
2.1	Chemicals	29
2.2	Experiments and equipments	29
2.2.1	Chemical precipitation	29
2.2.2	Solvent extraction	30
2.2.3	Ion Exchange	31
2.3	Modeling.....	31
2.3	Synthesis of OMS materials	34
2.4	Analysis	34
2.4.1	Titrations	34
2.5.2	Spectroscopic and chromatographic methods	35
2.4.3	Physical characterization.....	35
3.	RESULTS AND DISCUSSION	37
3.1	Precipitation of manganese and iron	37
3.2	Acid leaching of manganese concentrate	44
3.3	Separation of manganese by solvent extraction.....	44
3.4	Octahedrally coordinated manganese oxide materials	49
3.4.1	Synthesis and characterizing of OMS materials.....	49
3.4.2	Ion exchange properties	51
3.4.3	Metals separation with silica supported OMS-1 and OL-1.....	55
4	CONCLUSIONS.....	57
	REFERENCES.....	59

LIST OF PUBLICATIONS

- I Pakarinen, J., Paatero, E., Recovery of manganese from iron containing sulfate solutions by precipitation, *Minerals Engineering*, 24 (2011), 1421 - 1429.
- II Pakarinen, J., Paatero, E., Effect of temperature on Mn-Ca selectivity with organophosphorus acid extractants, *Hydrometallurgy*, 106(3 - 4) (2011), 159 - 164.
- III Koivula, R., Pakarinen, J., Sivenius, M., Sirola, K., Harjula, R., Paatero, E., Use of hydrometallurgical waste water as a precursor for the synthesis of cryptomelane-type manganese dioxide ion exchange material, *Separation and Purification Technology*, 70(1) (2009), 53 - 57.
- IV Pakarinen, J., Koivula, R., Laatikainen, M., Laatikainen, K., Paatero, E., Harjula, R., Nanoporous manganese oxides as environmental protective materials – Effect of Ca and Mg on metals sorption, *Journal of Hazardous Materials*, 180 (2010), 234 - 240.
- V Laatikainen, K., Pakarinen, J., Laatikainen, M., Koivula, R., Harjula, R., Paatero, E., Preparation of silica-supported nanoporous manganese oxide, *Separation and Purification Technology*, 75 (2010), 377 - 384.
- VI Pakarinen, J., Laatikainen, M., Sirola, K., Paatero, E., Koivula, R., Harjula, R., Behavior of silica-supported manganese oxides in hydrometallurgical separations, *Separation Science and Technology*, 44 (2009), 3045 - 3074.

AUTHOR'S CONTRIBUTION

The author has been the main author of the scientific articles I, II, IV and VI. Article III was done in cooperation with the Laboratory of Radiochemistry of University of Helsinki (UH) and was written by Doc. Risto Koivula. The author synthesized the studied OMS materials and was also a part of the studying group in Article V, which was written by Dr. Katri Laatikainen. Markku Laatikainen (Lic.Sc.) has been the main scientific advisor for the author in ion exchange studies and computational modelling (Articles IV and VI). He has also shared his advice and knowledge, in preparing the research plan and interpreting the experimental results. Professor Erkki Paatero has been the supervisor of all articles and he has given his experience throughout the studies.

In addition to published scientific articles, the author has presented some of the results covered in this thesis also at two conferences (Pakarinen, 2006) and (Pakarinen and Paatero, 2007). The author has taken the main responsibility for the study throughout the research.

SYMBOLS

A^+	univalent counter-ion
b_m	mass transport parameter, 1/s
BV	bed volume, mL
c	concentration, mol/L
d	average diameter of OL-1 crystals, m
D_m	micro-crystalline diffusion coefficient, m^2/s
D_{ax}	axial dispersion coefficient, m^2/s
F	Faraday constant
h_i	empirical parameter, -
I_c	ionic strength, mol/L
J	ion flux, $mol/(m^2s)$
k_{dis}	rate constant of the disproportionation reaction, $mol/(Ls)$
K_{dis}	equilibrium constant of the disproportionation reaction, -
L	average length of the OMS crystals, m
m	potential parameter, -
N	number of cations, -
p	heterogeneity parameter, -
q	amount of adsorbate in the solid phase, mol/kg
q_{max}	total amount of ion exchange sites, mol/kg
r_{dis}	rate of the disproportionation reaction, $mol/(Ls)$
R	gas constant, 8.314 J/(mol K)
t	time, s
T	temperature, K or °C
u	interstitial velocity, m/s
V	volume, L
x	axial coordinate, m
y	diffusion coordinate, m
z	ion charge, -
\square	empty vacant site

Greek letters

α, β, γ	reaction orders, -
γ_i	activity of component i, -
ε_b	bed porosity, -
ε_p	intra-particle porosity, -
ε_{tot}	total bed porosity, -
κ	affinity constant, L/mol
η	volume fraction of micro-crystals in the bed, -
μ	chemical potential, J/mol
ρ	density, kg/L
φ	electric potential, V
ν	stoichiometric coefficient, -

Subscripts and Superscripts

b	non-specific binding
feed	feed value
H	proton
i, j	ion
init	initial value
liq	liquid phase
p	pore
s	solid phase
sp	specific binding
0	initial value
e, f, r	disproportionation coefficients

ABBREVIATIONS

AOS	Average oxidation state
CMD	Chemical manganese dioxide
CP	Chemical plant
D2EHPA	Di-(2-ethylhexyl) phosphoric acid
DI	Deionization
EMD	Electrolytic manganese dioxide
EW	Electro winning
HC	High carbon
ICP-AES	Inductive coupled plasma-Atomic emission spectrofotometer
IX	Ion exchange
LC	Low carbon
MC	Medium carbon
NICA	Non ideal competitive adsorption
NMD	Natural manganese dioxide
OMS	Octahedral molecular sieve
OL	Octahedral layer
PLS	Pregnant leached solution
Redox	Reduction oxidation
SX	Solvent extraction

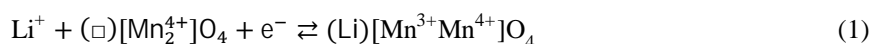
1 INTRODUCTION

This thesis is about the recovery and refining of manganese in hydrometallurgical processes. The Sections 1.1 – 1.3 give the background of manganese, a review of its occurrence, its known extraction processes, and its use in different applications. The scope of this thesis is given in the Section 1.4.

1.1 History and use of manganese

Manganese has a significant role in nature and in the activities of human being in modern world. Increased construction and greater consumption of industrial products are the main reasons for the expanded need of manganese. The main application of manganese is stainless steel (consumes more than 90% of the total mined manganese), where the role of Mn is to increase steel tenacity and hardness by binding and oxidizing the impurities like sulfur and phosphorus. Sulfur and phosphorous are impurities that make steel brittle and are originated from the iron ore. The property of manganese to eliminate these impurities was found in 1856 when the first iron and manganese alloy was made in *Bessemer* process using ferromanganese as an additive (Weiss, 1977). Mn is also used in steels to replace more expensive metals like Ni (Weiss, 1977). The amount of Mn in stainless steels is typically 1 - 2%. In austenitic manganese steels the amount could be as high as 12% (Johnson, 2003), (Kroschwitz and Howe-Grant, 1982), (Elvers *et al.*, 1990). In addition about 2% of manganese is used in different copper or aluminum alloys (Elvers *et al.*, 1990).

The second most significant manganese application (after metal alloys) is batteries consuming about 5% of mined manganese. The function of manganese (MnO₂, pyrolysite, early known as *magnesia negra*) in batteries is based on its good redox properties, which are involved in the charge transfer and/or prevent hydrogen gas evolution when battery charging. Manganese is used in several different battery types from NiCd to the batteries based on Li-ion technology. The Li⁺ ion involving redox reaction of manganese oxide is according to Eq. (1) (Feng *et al.*, 1999). The reaction goes right when charging and left when discharging, respectively. The oxidation reaction of hydrogen gas is according to the Eq. (2).



Here, the \square symbol means a vacant site.



The wet galvanic cell using pyrolysite as oxidizer was invented in 1860 and has become the basis of the modern electric cell industry and is still the largest non-metallurgical application of manganese (Weiss, 1977). Naturally occurring Manganese Dioxide (NMD) was used in batteries in past, but with increased specifications today, high purity Electrolytic Manganese Dioxide (EMD) is favoured instead of Chemical Manganese Dioxide (CMD) or (NMD) for the electrolytic cell materials (Pakarinen, 2006).

The function of MnO₂ in batteries is based on its favourable redox properties. MnO₂ materials have, however, also ion exchange properties, which make them promising inorganic adsorbent for several metals. With increased concern about the environment, attempts are being made to minimize the impact of human activity on the natural world. Worldwide, mining operations handle several million tons of metal solutions annually involving risk of environmental damage as a result of leaks in solution handling or poor tailings management. Inorganic material like bentonite has been used to protect environment around the places, where different chemical are transported or handled (Jan *et al.* 2007) and (Arcos *et al.*, 2008). On the other hand manganese oxide material called as Octahedral Molecule Sieve (OMS) have already been utilized in removal of radio nuclides in nuclear power plants and several studies have proved the materials being promising for separation of for example Cs, Sr, and U (Dyer *et al.*, 2000), (Runping *et al.*, 2007), (El Absy *et al.*, 1993). The ion exchange and redox properties of MnO₂ materials in hydrometallurgy are discussed more detailed in the Section 3.4 and in the Articles III - VI.

The contribution of the name manganese (*mangania* in Greek origin meaning magic) to real life is rather apropos due to the rich phenomena of manganese in chemistry and biochemistry (Weiss, 1977). The minor applications of manganese are use as catalyst, oxidizer in organic synthesis and as pigment in paint, glass and ceramic industry. In addition manganese is an essential nutrient for plants and animals and is therefore added as MnSO₄ in fertilizers and animal foods (Greenwood, 1984). The requirements or typical concentrations for different manganese products are shown in the Table 1. In addition to the impurity content, the requirements for physical and mechanical properties depend on the application of each material.

Table 1 Concentrations of elements in manganese products (Elvers *et al.*, 1990)

Element	concentration, ppm (% Mn)			
	Mn metal	EMD (grade 1)	MnCO ₃	MnSO ₄ H ₂ O
Mn	> 99.7 %	> 59%	> 40%	> 31.8%
Al	a	100	100	a
As	a	1	a	5
Cd	a	1	100	1.5
Co	10	1	100	a
Cr	a	1	100	a
Cu	10	1	100	a
Fe	10	10	a	40
Na	a	a	300	a
Ni	10	1	100	a
Pb	a	7	a	15
Se	5	a	a	a
Zn	a	1	a	500

a: Value was not found

1.2 Occurrence and mining of manganese ores

Manganese is the 12th abundant element in the Earth's crust. The most of the manganese is deposited as pyrolusite (MnO_2) in the southern hemisphere of the Earth. Only ores containing > 35% Mn are regarded as manganese ores. Ores containing 10 - 35% manganese are classified as ferruginous manganese ores and ores containing 5 - 10% manganese as manganiferrous ores (Elvers *et al.*, 1990). All industrially significant manganese deposits are sedimentary origin, which are formed by precipitation, a result from combining with oxygen, hydroxide or carbonate. The largest depositions are located in the Republic of South Africa, Australia, Brazil, Gabon and Ukraine which are also the biggest manganese producing countries, respectively. Significant resources of manganese together with nickel and cobalt occur on the floor of oceans (Johnson, 2003), (Elvers *et al.*, 1990), (Havlik *et al.*, 2005). In addition to the main deposits, manganese is also found bounded with several metals or metal compounds like nickel laterite, silicate or sulfide (etc. Zn sphalerite) ores (Acharya and Nayak, 1998). Due to the rather high reducing potential of manganese (Mn^{3+} to Mn^{2+} is 1.5 V), it dissolves in leaching and ends up to hydrometallurgical process solution together with the base metals. Due to the increased awareness today, a significant amount of Mn is utilized from recycled metal waste (batteries, spent electrodes, catalyst, steel scraps, sludges etc.) (Pakarinen, 2006), (Zhang and Cheng, 2007), (de Souza and Tenório, 2004).

1.3 Uptake and processing of manganese

Manganese oxides were the only known and used manganese compounds until the 18th century. Before that, MnO_2 was applied as pigment in making glass and ceramics. In 1774 *Johann Ghan* succeeded in isolating metallic manganese from pyrolusite using charcoal as reducing material. The same mechanism is still carried out in pyrometallurgy making ferromanganese (Weiss, 1977). In hydrometallurgy several separation methods based on chemical precipitation, solvent extraction and electrolysis to process manganese are in use today.

Manganese is the fourth most used metal after iron, aluminium and copper and its total mined amount in 2009 was 11.3 Mt (Anonym., 2009). The methods and technology employed for the mining of manganese ore vary depending on the ore size, deposition, concentration, type, available reagents, planned end use etc. The most used technologies to mine manganese ore are opencast and underground techniques.

1.3.1 Pyrometallurgy

In pyrometallurgy metals or metal alloys are refined and/or produced at elevated temperature using oxidation or reduction. Heating and refining of primary material are made in blast furnaces using only coke as reductant and as energy source or in electric smelting furnaces. Depending on the ore quality the efficient electric furnaces consume about 2100 - 2800 kWh electric power per 1 t of ferromanganese alloy (Kroschwitz and Howe-Grant, 1982) and (Elvers *et al.*, 1990). Reduction with carbon (coal) or silicon is the method to produce ferromanganese (FeMn) with high carbon (HC), medium carbon (MC) or low carbon (LC) content or siliconmanganese (SiMn) intermediates for steel industry. The temperature required for complete reduction of manganese (Eq. 3) is high (1267°C) owing to the stability of the MnO compound (Kroschwitz and Howe-Grant, 1982) and (Elvers *et al.*, 1990). Pyrometallurgical methods can be applied only for high-grade ore with low impurity content. Phosphorus and

arsenic content are very critical and their weight percentage in the feed of smelting should not exceed 0.5%. Other compounds that are critical to the quality of the metal product are Al₂O₃, SiO₂, CaO, MgO, and S (Elvers *et al.*, 1990). Pyrometallurgy is applied to convert the sparingly-soluble ore to a more soluble form to promote leaching. In Eq. (4) the roasting of very low solubility sulfide mineral to more acid soluble oxide is shown.



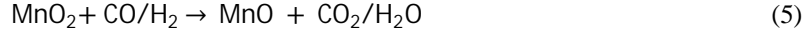
Equations 3 and 4 show the drawback of pyrometallurgy in the view of environment and people. Both reactions (carbon refining and roasting) produce toxic greenhouse gases. The SO₂ problem has, however, been solved by technology, where SO₂ is converted by a catalytic oxidation method to H₂SO₄, which is a commonly used reagent in chemical industry. More problematic are CO and CO₂, as their capture and storage decreases the efficiency and economy of the process. Different capturing methods are being studied widely in order to drive the metal industry towards sustainability.

1.3.2 Hydrometallurgy

Leaching is the method, where the metals from ore mineral calcined or roasted concentrates, or recycled materials is converted into dissolved species. This is the beginning of hydrometallurgy. The history of hydrometallurgy as industrial metal processing is not as long as that of pyrometallurgy, but the importance of hydrometallurgy in metal processing has been steadily increasing. The need for more effective, flexible and selective method to recover metals from low grade, complex and small-body ores is the reason for the increasing importance of hydrometallurgy. All this is a consequence of the fact that most of the rich ore bodies are already utilized. The quality of raw material for metallurgical industry is getting poorer and they are becoming more difficult to process. The processing of complex and low-grade ores by conventional pyrometallurgical methods is not possible.

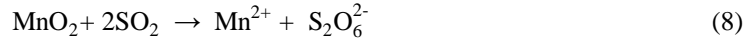
Adjectives like selectivity, flexibility, and environment friendly describe the properties of hydrometallurgical methods compared with pyrometallurgy. Productivity is, however, usually slower due to the relatively slow mass transfer in aqueous solutions. The studies in ore leaching and selective metal uptake in hydrometallurgy have led to breakthroughs in the process of many metals and made possible to recover economically new, low-grade ore deposits.

The type of ore has a critical effect on the leaching process and chemicals to be used. A great part of manganese in ore is at oxidation state 3+ or 4+ and needs reduction in order to dissolve. Ore can be pre-treated by pyrometallurgical methods by smelting, reduction-roasting, sulfatizing, and chloridizing. Typically, the recovery efficiencies in manganese leaching processes are between 90 - 98% (Zhang and Cheng, 2007). Smelting and reduction-roasting at elevated temperature (about 700 - 900°C) followed by sulfuric acid leaching is by far the most commonly used method in the manganese industry for production of intermediate or final manganous sulfate. Hydrogen gas, charcoal or other carbon containing material can be used as reductant (Eq. 5 and 6) (Zhang and Cheng, 2007).

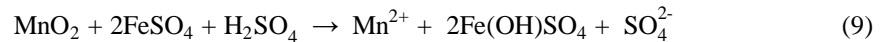


Sulfatizing is a method to convert MnO_x compound to a more soluble form. H_2SO_4 , $(\text{NH}_4)_2\text{SO}_4$ or SO_2 are used as sulfatizing agents but SO_2 is the most used due to the economy, easy manufacturing, fast kinetics, low temperature operation, ease of purifying the leach liquor and elimination of barren solution disposal problem (Vu *et al.*, 2005). Sulfatizing roasting followed by water leaching has been investigated for recycling of zinc-carbon spent batteries with a production of manganese and zinc sulfates (Abbas *et al.*, 1999). Compared with pure hydrometallurgical processes, combining pyro-hydrometallurgical treatments yield better results for efficient recovery of metals from poly-metallic manganese nodules (Kohga *et al.*, 1995). Due to the need for heating the energy consumption is higher than in pure hydrometallurgical method.

H_2SO_4 , SO_2 or $(\text{NH}_4)_2\text{SO}_4$ are the most used leaching chemicals for manganese ore. Also the dithionate process is studied to recover manganese from low-grade ores (Ravitz *et al.*, 1946). Similar to pyrometallurgy SO_2 is the most widely used leaching chemical for manganese in hydrometallurgy. Reduction and leaching of manganese at high oxidation state with SO_2 can result in different solutions depending on the conditions and ore material (morphology, Mn/O ratio etc.) (Eqs. 7 and 8) (Senanayake, 2004a) and (Senanayake and Das, 2004b).



The advantage of the latter process is the formation of dithionate, which stabilize both the reduced Mn(II) and calcium in solution, while extra calcium is precipitated as CaSO_4 precipitate. Several other reducing agents in leaching have been studied and used in real processes. Iron at oxidation state 2+ effectively reduces Mn^{4+} under slightly acidic conditions according to the Eq. (9) (Zhang and Cheng, 2007), (Vu *et al.*, 2005) and (Das *et al.*, 1982).



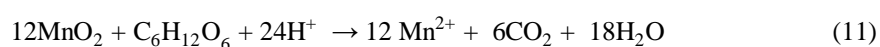
Reduction of Mn^{4+} with strong acid leads to better Mn leaching recovery but it also increases the amount of soluble iron sulfate according to Eq. (10).



The drawback of using FeSO_4 as reducing agent is the need for purification of the leaching solution from dissolved iron, which increases production costs and the amount of side material. One opportunity is to use ammonia-ammonium solution together with FeSO_4 , since Fe forms a stable ferrous ammine complex at the pH range from 9.5 to 9.8. Iron can be oxidized and precipitated as ferric oxo hydroxide by MnO_2 , while Mn is reduced to Mn^{2+} and is stabilized in the solution as ammine complex.

Simultaneous leaching of manganese oxide and metal sulfides has been studied widely by (Kholmogorov *et al.*, 2000), (Yaozhong, 2004), (Thomas and Whalley, 1958) and (Lu and Zou, 2001). In this method, sulfide ion acts as reductant, while manganese oxidizes. The studied minerals are galena (PbS), sphalerite (ZnS), zinc matte, pyrite (FeS₂), nickel matte, and pyrite-ferrous lignite. The key operation parameters were found to be the MnOx/MeS ratio, acid concentration, temperature and leaching time.

Several carbohydrates like sugars, acids or even wood from industrial waste streams have been used as reductant for manganese oxide ore. The stoichiometric reaction with glucose in acidic conditions is according to Eq. (11).



Elsherief (2000) has studied electro-reductive leaching of low-grade manganese ore in sulfuric acid media. The redox potential of solution was scanned from anodic to cathodic potential and the leaching of MnO₂ was monitored by voltammograms.

Leaching in autoclaves using reagents with strong concentration ($c > 1\text{M}$), high temperature ($T > 100^\circ\text{C}$) and pressure ($p > 1 \text{ bar}$) make the redox reactions taking places with increased kinetics. Leaching recoveries of $> 95\%$ can be obtained in a few hours. The manganese recovery from the ore with low concentration is, however, not economic when using such amount of reagents and energy. The advantages of the bioleaching process include the absence of noxious off-gases or toxic effluent, simplicity of plant operation and maintenance, economic and simple process requiring low-capital and low-operating costs, and applicability to various metals. The leaching kinetics is, however, much slower than in the chemical leaching methods. Bioleaching methods for several metals (Cu, Au, Ag, Ni, Co, Zn, Mn, and Li) and ore minerals (e.g. chalcopyrite, pyrite, sphalerite, laterite and pyrolusite) or recycling materials have been studied (Brierley and Brierley, 2001), (Rawlings, 2002), (Acharya *et al.*, 2003), (Le *et al.*, 2006), (Lee *et al.*, 2001), (Cameron *et al.*, 2009), (Frías, 2002), (Xin *et al.*, 2009) and commercial processes for the recovery of gold, copper and nickel are applied (Brierley and Brierley, 2001), (Morin *et al.*, 2006), (Watling, 2006). Similar techniques for low-grade nickel sulfide ores are studied by (Halinen *et al.*, 2009), (Rawlings, 2002), (Watling, 2006). Depending on the acceptor of electrons in the metabolism of microbes, bioleaching is divided into direct and indirect methods (Lee *et al.*, 2001). The leaching of the metals is a consequence of the microorganisms that grow in aerobic or anaerobic conditions oxidizing sulfide (or indirectly ferrous ions to ferric, which oxidizes sulfide to sulfate) or reducing oxide minerals (Acharya *et al.*, 2003), (Halinen *et al.*, 2009). In both cases the biological process needs the presence of organic carbon and energy sources. Illustrations of different leaching methods with varying chemical and energy consumption are shown in the Fig. 1. Time and volume of reaction and used method depend on the ore concentration.

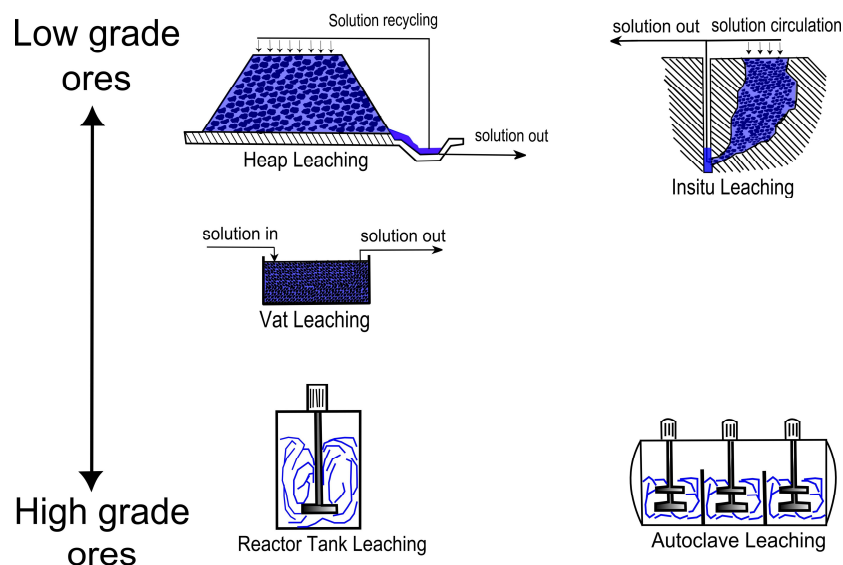


Figure 1. Leaching methods with varying chemical and energy consumption.

Due to the increased amount of recycling today, a great amount of manganese is recovered from different electrical disposals. One increasing source are batteries, which are widely studied (Nan *et al.*, 2006), (Kim, 2009), (Sayilgan *et al.*, 2010) in a view of manganese recovery as Zn-Mn ferrites or as $MnSO_4$. Depending on the type of battery, the amount of Mn can vary between 25 - 45%. Comparing this to the natural ore, where the content of manganese can be up to 75% (in pyrolusite), the content is low. In addition the collection of batteries needs effective logistics. One more challenge with recycling has also been the heterogeneity of materials, that needs several physical (sorting, dismantling, magnetic separation, and grinding), and chemical (pyro- and hydrometallurgical) pre-treatments for metals recovery (Sayilgan *et al.*, 2009). The increased concern about the environment and the legislations (The European Union Directive 2006/66/EC), however, force the amount of recycling to be increased. Several commercial companies are recycling batteries and accumulators.

The sulfate process is favored in hydrometallurgy due to the better economy (lower price of H_2SO_4 or SO_2 compared to for example HCl , HNO_3 and H_3PO_4). The sulfate solution is less corrosive and no poisonous gas is formed in electrolysis (compared to e.g. chloride media). The choice of solution media and the condition is very critical, due to the complex interactions between dissolved ions and water molecules (complex forming, coordination, solvation, precipitation). The properties of leached solution (PLS) affect the metal recovery and the choice between different purification processes including chemical precipitation, cementation, solvent extraction, ion exchange, adsorption, and electrolysis. Also membrane separation and crystallization can be used in some specific cases but their industrial use is quite minimal. Since the treatment of impurities usually mean extra processing stages, the evaluation of the process alternatives is very important. The methods are briefly and in general described below and their advantages, disadvantages and applications especially involved in the manganese refining are discussed detailed in further.

Recovery of manganese with precipitation

The Eh-pH diagrams for metal compounds (calculated in this study for Mn-Fe-S system in Fig. 4) show essential knowledge about the equilibrium behaviour of ions in solution as a function of pH and redox potential at chosen temperature (25°C). This knowledge is utilized in leaching and precipitation in order to choose the right conditions and chemicals for the desired reactions (Article I). The understanding of the behaviour of ionic compounds through the hydrometallurgical process is important in order to avoid the unwanted precipitation or by-product formation. The theoretical phase boundaries give, however, only an approximate behaviour of the multi component system.

Hydroxide precipitation is one of the most used precipitation method to recover metals from the liquid phase. The selectivity of hydroxide ions on individual metal cation against the others having same oxidation state is, however, not very good. For example iron at oxidation state 2+ is not possible to be separated from Cu, Co, Ni, Zn and Cd (Monhemius, 1977). The selectivity can, however, be increased by increasing the oxidation state of ion (Article I). Iron oxidation with molecular oxygen was assumed to follow the mechanism published by (Zhang *et al.*, 2000b) and is affected by partial pressure of oxygen. The sum reaction is shown in the Eq. 12. Iron at the oxidation state of 3+ precipitates selectively from manganese due to the very low value of solubility product ($2 \cdot 10^{-39}$). Depending on the precipitation conditions, different ferric oxo hydroxides (α -FeOOH, β -FeOOH or α -Fe₂O₃) (Loan *et al.*, 2006) can be formed (Eq. 13).



The pK_a values (*) were calculated using HSC 6.1. The ions at oxidation state 3+ have much lower solubility than the ions at oxidation state 2+, making hydroxide precipitation a feasible method to purify metal solution from iron, for example, when the redox potential of solution is suitable. The solubilities of metal hydroxides on the pH scale can be calculated using Eq. (14). In this work (Article I) the values of K_S are obtained from Lange's handbook of chemistry (Dean, 1999).

$$\log[K_S] = \log[\text{Me}^{n+}] + n\log[\text{OH}^-] \quad (14)$$

Here K_S is the solubility product between metal and hydroxide ions and n is the oxidation state of the metal ion, respectively. Oxidation of iron in order to intensify the separation is generally used in the metal's refineries. Decreased solubility of metal ion by oxidation makes also the other precipitation methods (e.g. carbonate) more effective. Strictly thinking due to the decreased hydroxide solubility the used separation method is a combination of two different precipitation mechanisms (hydroxide and carbonate precipitation) (Article I). The oxidation states for metals in solution as a function of pH and oxidation potential can be seen in Eh-pH (Pourbaix) diagrams (Fig. 4). Industrially used separation methods for iron removal follow jarosite AFe₃(SO₄)₂(OH)₆, goethite FeOOH, paragoethite or as hematite Fe₂O₃ mechanisms (Loan *et al.*, 2006). The alternative cations A can be K⁺, Na⁺, Li⁺, NH₄⁺, or H₃O⁺ (Claassen *et al.*, 2002). Temperature, solution pH and redox potential of the system has to be under control in order to have iron removal with good functionality (Fig. 2, (Claassen *et al.*, 2002), (Söhnel and Garside, 1992)). The control of leaching may be difficult due to the complicated reaction mechanism (Stott *et al.*, 2000), (Halinen *et al.*, 2009).

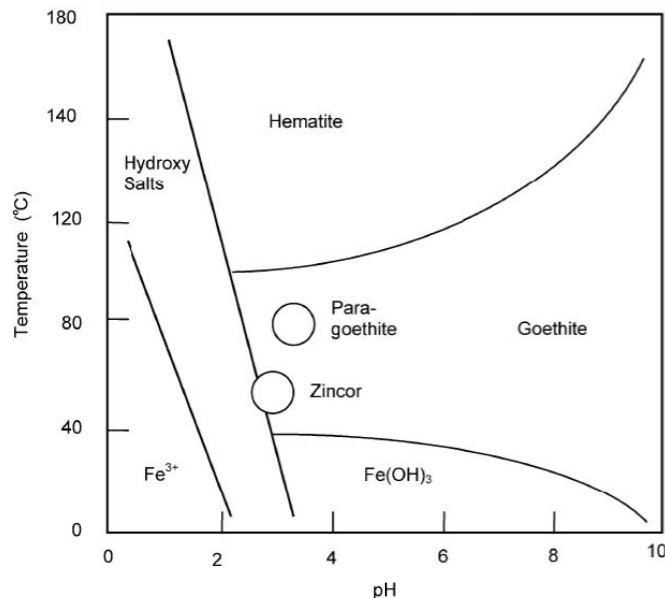


Figure 2. Effect of solution pH and temperature on the forming of iron precipitates (Claassen *et al.*, 2002).

Oxidation potential of Mn and Fe decreases and the reaction kinetics becomes faster with increasing pH (decreasing H^+ ion activity). This property is utilized by pre-neutralizing the solution before iron oxidation with O_2 or manganese oxidation with the SO_2/O_2 gas mixture. The applied metal precipitation using a combination of Eh-pH and solubility diagrams are discussed in more detail in the Section 3.1.

Solid-liquid separation is very important unit process in hydrometallurgy. Poorly operating separation can be a bottle-neck of the process leading to slow residence time, low yields, high operation costs or poorly running process. The size of particles in precipitate affects the settling property and filterability. The particle size is dependent on the super-saturation of the specific species in solution and temperature. The particles with slow crystal growth are bigger than those with fast growth. Goethite for example has a highly crystalline $\alpha\text{-FeO} \cdot \text{OH}$ and a poorly crystalline $\beta\text{-FeO} \cdot \text{OH}$ forms depending on the crystal growth kinetics (Claassen *et al.*, 2002), (Ismael and Carvalho, 2003).

The separation of base metals (Cu, Zn, Ni and Co) from manganese can be done selectively using sulfide precipitation at pH below 4. The precipitation lines of metal sulfides and activity of sulfide ion as a function of solution pH can be calculated according to (Monhemius, 1977). For a comparison the measured metal ion concentrations in equilibrium with solution pH and sulfide ion activity were plotted as well. The sulfide ion activity was calculated according to the Eq. (15), where the pressure of H_2S gas is specified to be 1 bar. Calculations of the solubility products of several base metals indicate the possibility to separate these metals from manganese using sulfide precipitation. In practice, however, good selectivity is not always possible due to the mass transfer problems in reagent feed (Article I). The concentration close to the feed is

always higher than farther in bulk solution, causing co-precipitation of unwanted metals. The activity of carbonate ion can be calculated according to Eq. (16) (Ringbom, 1963).

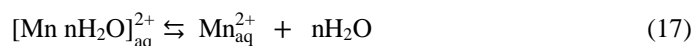
$$\log[K_S] = \log[S^{2-}] + 2\log[H^+] , \quad \text{where } \log[K_S] = 20.9 \quad (15)$$

$$\log[K_S] = \log[CO_3^{2-}] + \log[H^+] - \log[HCO_3^-] , \quad \text{where } \log[K_S] = 10.3 \quad (16)$$

Coordination in aqueous solution

Coordination of compounds is based on the donor-acceptor property of anion (Lewis base) and metal cation (Lewis acid). This phenomenon is always present in hydrometallurgy, especially in metal separation, where the different ability of metal ions to coordinate with organic and inorganic anion is utilized. Typical anions that form complexes with metal ions are shown in Table 2 (Habashi, 1999). Most of these anions are used in organic extractants as active group. The strongest complex formers are NH_3 , CN^- , and Cl^- , which also form aqua soluble complexes with several metal cations. Due to the polar nature of ions and dipole character of water molecule, ions in aqueous solution are coordinated with the water molecules around them. The amount of water molecules coordinated on the primary sphere of metal is called solvating number. The solvating energy of ions plays a major role in thermodynamics of ion interaction in aqueous solution. For example the total heat of redox reaction between manganese oxide and ferrous iron is the sum of heats of solvating of MnO_2 and Fe^{2+} .

The water replacement from the ion coordination sphere is a result of the interaction of metal ion with the electron donor and the tendency of the system to reach the minimum energy state. The replacement of hydration water from Mn^{2+} ion is shown in Eq. (17).



The reciprocal interaction of ions in solution affects their activity. If the concentration of ions in solution increases, the electrostatic forces between the ions become more significant and their activity coefficients (γ_i) decreases less than unity. In other words, solution behaves more like non-ideal (Snoeyink and Jenkins, 1980). Non-ideal behavior of solution is a consequence of high ionic strength. Ionic strength of solution can be calculated by Lewis and Randall (Snoeyink and Jenkins, 1980) (Eq. 18), when the dissolved components and their concentrations are known.

$$I_c = \frac{1}{2} \sum_i c_i z_i^2 \quad (18)$$

Here c_i is the concentration of species, i and z_i is its charge. In concentrated solutions, where the behavior of ions is not ideal, it is useful to use the activity coefficients of components instead of concentrations when doing calculations. There is a relation between ion activity and ionic strength of solution and several approximations between ion activity and concentration are made. In solution with low ion strength, widely known approximation is so called Debye-Hückel limiting law (Eq. 19). This approximation is valid, when the ionic strength is less than $5 \cdot 10^{-3}$ mol/L (Pitzer, 1991), (Snoeyink and Jenkins, 1980).

$$-\log(\gamma_i) = \frac{1}{2} z_i^2 \sqrt{\mu} \quad (19)$$

The oxidation state has more significant effect on the characteristics of ion (ion activity) than the chemical potential has (Article I). The higher the ion valence is, the higher also its polar nature and this increases the attractive interaction between the ions with opposite sign and water molecules. The repulsive interaction between ions with the same sign increases, respectively. The relation between ion activity and concentration are described elsewhere with the models of Pitzer (Pitzer, 1991).

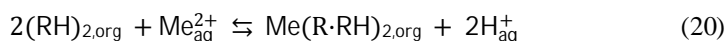
Table 2 Ionic metal complexes with different anions (Habashi, 1999).

	NH ₃	CN ⁻	Cl ⁻	F ⁻	OH ⁻	S ²⁻	SO ₄ ²⁻	CO ₃ ²⁻
Ag ⁺	Ag(NH ₃) ₂ ⁺	Ag(CN) ₂ ⁻	AgCl ₂ ⁻					
Al ³⁺				AlF ₆ ³⁻	Al(OH) ₄ ⁻			
As ³⁺						AsS ₃ ³⁻		
As ⁵⁺						AsS ₄ ³⁻		
Au ⁺	Au(NH ₃) ₂ ⁺	Au(CN) ₂ ⁻						
Au ³⁺			AuCl ₄ ⁻					
Be ²⁺				BeF ₃ ⁻	Be(OH) ₃ ⁻			
Co ²⁺	Co(NH ₃) ₆ ²⁺	Co(CN) ₆ ⁴⁻						
Co ³⁺	Co(NH ₃) ₆ ³⁺	Co(CN) ₆ ³⁻						
Cu ⁺	Cu(NH ₃) ₂ ⁺	Cu(CN) ₂ ⁻	CuCl ₂ ⁻					
Cu ²⁺	Cu(NH ₃) ₄ ²⁺		CuCl ₃ ⁻					
Fe ²⁺		Fe(CN) ₄ ⁴⁻						
Fe ³⁺		Fe(CN) ₆ ³⁻					Fe(SO ₄) ₂ ⁻	
Hg ²⁺	Hg(NH ₃) ₂ ²⁺	Hg(CN) ₄ ²⁻	HgCl ₄ ²⁻			HgS ₂ ²⁻		
Mn ²⁺		Mn(CN) ₆ ⁴⁻						
Nb ⁵⁺				NbF ₇ ²⁻				
Ni ²⁺	Ni(NH ₃) ₆ ²⁺	Ni(CN) ₄ ²⁻						
Pb ²⁺			PbCl ₄ ²⁻		Pb(OH) ₃ ⁻			
Pt ⁴⁺			PtCl ₆ ²⁻					
Sb ³⁺					Sb(OH) ₄ ⁻	SbS ₃ ³⁻		
Sb ⁵⁺					Sb(OH) ₆ ⁻	SbS ₄ ³⁻		
Si ⁴⁺				SiF ₆ ²⁻				
Sn ⁴⁺			SnCl ₆ ²⁻		Sn(OH) ₆ ²⁻	SnS ₃ ²⁻		
Ta ⁵⁺				TaF ₇ ²⁻				
UO ₂ ²⁺							UO ₂ (SO ₄) ₃ ⁴⁻	UO ₂ (CO ₃) ₃ ⁴⁻
Zn ²⁺	Zn(NH ₃) ₄ ²⁺	Zn(CN) ₄ ²⁻			Zn(OH) ₅ ⁻			

The chloride ion is much stronger complex former than sulfate ion. Like cyanide it forms anionic complexes with several metal cations. This is utilized in e.g. ion exchange (solvent extraction) with anion exchangers, which makes coordination bonds with metal chloro-complexes. More effective leaching of HCl compared to H₂SO₄ is explained by more stable metal-chloro-complexes than metal-sulfate complexes, and also because the activation energy of metal ions in chloride solutions is lower compared to sulfate solutions (Lu and Zou, 2001). Metals are classified as hard, soft or intermediate by their characteristics to make complexes with different donor atoms (Lewis bases). Metal ions classified as soft (b type) prefer to complex with less electronegative donor atoms like N, P, and I, whereas the cations classified as hard complex preferable with more electronegative donor atoms like F, Cl and O. According to Martell and Hancock (1996), Mn²⁺ is classified as intermediate and has approximate six water molecules (n = 6 in Eq. 17) in the primary sphere in water solution. The solvated Mn complex has octahedral structure.

Recovery of manganese by solvent extraction

The hydration water of metal ion is involved also in solvent extraction, especially the coordination between the metal ion and organic ligand. Cations and anions are classified based on their ability to form complexes and the majority of complex formation follows the Eigen mechanism (Leeuwen, 2008), (Burgess, 1978). Ions prefer the complex with counter ions having the same characteristics. In order to form the metal-ligand bond, water molecules have to be released from the metal coordination sphere (dropping the coordination number). An organic ligand fills the gap in the coordination sphere and makes the covalent bond with the metal ion. The extraction equilibrium between the anhydrated metal ion in the oxidation state two and the extractant in H^+ form (dimer) is shown in Eq. (20).



The kinetics of ligand exchange and the geometry of the coordinated complex are affected by the ion charge and radius (Martell and Hancock, 1996). According to Burgess (Burgess, 1978), the ability of metal cations to release water molecules vary according to the nature of the cation. This can be the extraction rate determining step. In solvating systems the aqua molecules are transferred to the organic phase as hydrated to metal ions. This is characteristic of a reagent having oxygen bonded to carbon (ethers, esters, alcohols etc.) (Ritcey, 2006).

The separation of manganese from other transition metals in hydrometallurgy has been done using, for example, di-(2-ethylhexyl) phosphoric acid (the active compound in D2EHPA), bis-(2,4,4-trimethylpentyl) phosphinic acid (the active compound in CYANEX 272, a tertiary carboxylic acid (Versatic 10) or a synergistic system of Versatic 10 and α -hydroxyoxime reagents (Preston, 1999), (Tsakiridis and Agatzini, 2004), (Ndlovu and Mahlangu, 2008). The drawback of the Versatic 10/ α -hydroxyoxime system is that the hydroxyoxime suffers from instability (Swanson, 1977). D2EHPA has been used for manganese separation from cobalt (Feather *et al.*, 2000), (Zhang and Cheng, 2007), (Cheng, 2000), (Devi *et al.*, 2000) and is economically the best choice when Ca is not greatly present in the feed solution. D2EHPA is also a more acidic reagent (pK_a value of 3.9) than the others (6.2 for CYANEX 272 and 7.33 for Versatic 10) (Shan *et al.*, 2008), (Preston, 1994), which permits separations at lower pH, consequently avoiding neutralization of the leach solution. Temperature was shown to have a significant effect on Mn selectivity against alkaline earth metals (Ca and Mg) with D2EHPA (Article II).

Methods for the production of Mn products

The production of metallic manganese by electrolysis was studied as literature review (Pakarinen, 2006). In Articles III-VI the synthesis, characterization and binding of three types of OMS materials on silica are shown. The ion exchange properties and metal ion uptake from hydrometallurgical and environmental simulant solutions are shown and discussed as well.

1.4 Scope of the thesis

This thesis focuses on manganese recovery and refining from hydrometallurgical sulfate solution in order to produce manganese products by means of technically and economically favourable method. As one application for manganese, OMS materials with ion exchange properties were synthesized and studied. The electrolytic production of metallic manganese is not included in the experimental part. In order to have proper OMS material for different ion exchange application, the binding of OMS materials on silica was also done. All experiments concerning manganese recovery from multi-metal solution have also had industrial interest. Fig.1 shows a simplified process chart of the studies of this work (inside the dotted lines). Dashed (black) lines describe the pyrometallurgical and solid (blue) lines hydrometallurgical processing.

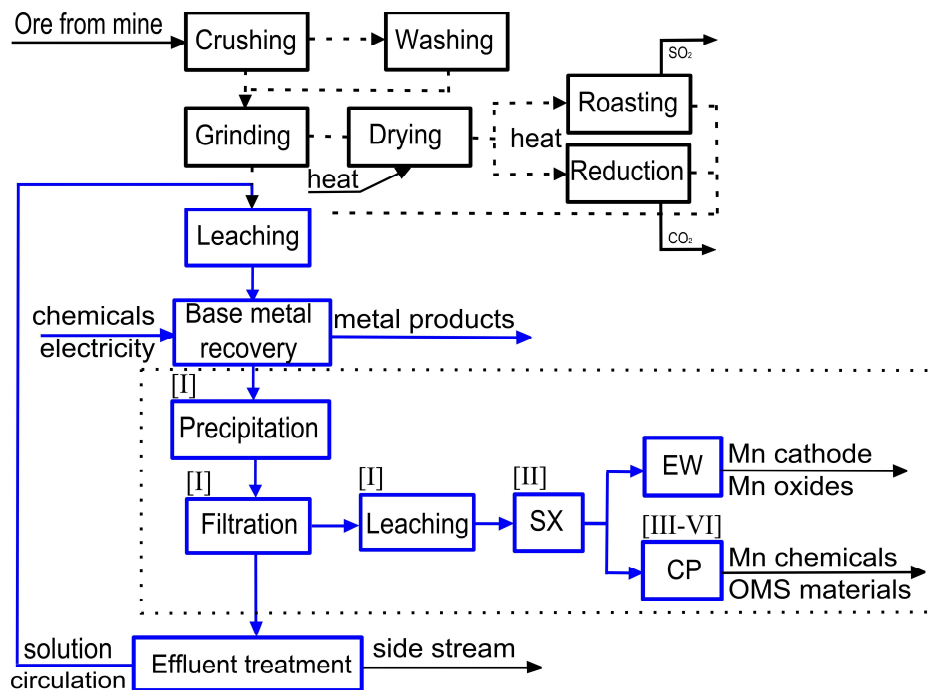


Figure 3. Principal block diagram of manganese refining in hydrometallurgical process. Dotted line and the Roman numerals correspond the topics of this thesis and the published articles. Abbreviations corresponds solvent extraction (SX), electro winning (EW) and chemical plant (CP).

This thesis does not give the answers to all questions concerning manganese recovery and refining from solution of any type and condition, but give valuable information about manganese recovery, processing methods, chemicals and conditions in sulfate media.

1.4.1 Objectives of the study

- i) To study and compare the precipitation methods with different reagents in order to recover manganese from multi-metal solution and remove iron impurity.
- ii) To find knowledge for the selection of extractant from two commercially manufactured and widely used phosphorus acid derivatives and optimize the extraction conditions in order to have very pure MnSO_4 solution for the production of electrolytic or chemical manganese.
- iii) To synthesize and characterize the OMS materials, their silica composites and to elucidate the behaviour and ion exchange properties of the materials in hydrometallurgical or a specific environmental applications.

1.4.2 New findings

The following results are believed to be found in this dissertation:

- i) Combined air oxidation with carbonate precipitation using limestone is technically and economically one of the most favourable separation method for iron and manganese.
- ii) Temperature has a great effect on Mn-Ca selectivity with Di-(2-ethylhexyl) phosphoric acid (D2EHPA) reagent. The subtraction of ΔpH_{50} values of Ca and Mn was increased by 0.65 pH units (more than doubled), when temperature was changed from 50 to 5°C.
- iii) Multi-metal tailings solution with low metal ion concentration can be utilized in synthesizing of nanoporous OMS materials with ion exchange properties.
- iv) Binding of OMS nanoparticles on silica can be done with rather simple method and reasonable metal capacities and selectivities for Cu, Cd, Ni, and K over Ca and Mg are attained with the materials.

2. EXPERIMENTAL

2.1 Chemicals

All synthetic metal solutions were made by dissolving analytical grade metal salts in deionized (DI) water. Solvent extraction experiments were carried out with diluted organophosphorus acid derivatives; di-(2-ethylhexyl) phosphoric acid (D2EHPA) from Lanxess and bis-(2,4,4-trimethylpentyl) phosphinic acid (CYANEX 272) from Cytec Industries Inc. The reagents were diluted to 25 vol-% with the aliphatic diluent Exxsol D-80 or D-60 from ExxonMobil Corporation. Commercial aqueous Ludox HS-40 (Grace Davison) silica sol was used as the binding agent in OMS experiments. According to the manufacturer (Grace Davison), silica content is 40 wt% and the average particle size is 12 nm. Density of amorphous silica solution is 1.295 g/cm³ at pH 9.4 and 25°C, and specific surface area is 198 - 258m²/g. Kieselgel 100 was obtained from Merck. B-MnO₂ was obtained from Riedel-de-Haan.

2.2 Experiments and equipments

All experiments were carried out in laboratory scale with volumes from 100 mL up to 20 L. The precipitations were done in semi batch system, where metals were precipitated by feeding the reagent in small portions (solid reagents) or continuously (gases, liquids or dispersions). All solvent extraction experiments were done batch wise in a glass reactor with a volume of 1L. The extraction equilibrium was adjusted by changing metal ion or hydrogen ion (pH) concentration in aqueous phase.

2.2.1 Chemical precipitation

The aim of precipitation experiments was to study the Mn recovery from the multi-metal tailings solution. Iron selectivity was also an essential property in view of the production of MnSO₄ solution with high purity. Five different precipitation chemicals were used. Carbonate precipitation was studied using NaHCO₃, Na₂CO₃ and CaCO₃. Hydroxide precipitation was done by using Ca(OH)₂ and oxidative precipitation using O₂/SO₂ gas mixture (Alternatively air from AGA Finland was used instead of O₂). All solid reagents were fed into the reactor as slurry with concentration of 200 g/L. Feeding was carried out by a tubular pump with varying flow rate from 0.5 to 3.5 mmol/min. The mass balance was controlled by weighing the feed slurry and analyzing periodically Na or Ca concentrations in the solution, respectively. The exact volumes were calculated from weighted mass and measured density (Anton Paar DMA 4500 apparatus). All experiments were carried out in batches. Oxidative precipitations with SO₂ were carried out in 1 L glass reactor, where the poisonous SO₂ was easier to control. Gases were fed through the calibrated rotameters (SHO Rate by Brooks Instrument B.V.) with glass pipes R-2-15-D for O₂ (air) and R-2-15-AA for SO₂.

Leaching

The leaching properties of hydroxide and carbonate precipitates were compared in regards to acid consumption to manganese and to leaching percentages. The metals from the primary precipitate were leached with sulfuric acid solutions at various concentrations. The effect of H₂SO₄ amount on manganese and iron leaching was studied. The effect of ammonium ions on leaching was also studied by dissolving (NH₄)₂SO₄ in acid solutions to meet the authentic

conditions of Mn anolyte. The leaching kinetics of MnCO_3 and FeCO_3 were studied in batch system for optimization of reagent consumption and reaction time.

Continuous manganese recovery

Continuous leaching of Mn from carbonate concentrate and iron precipitation was done in stirred tank reactors with volumes of 10 and 20 L, respectively. All experiments were carried out at 40°C. The MnCO_3 feed (200 g/L) to leaching was made in a separate semi continuous process using Na_2CO_3 as reagent. In the iron removal step air and CaCO_3 were continuously fed with the slurry from the leaching reactor. Air flow was monitored and adjusted using a calibrated rotameter. The CaCO_3 slurry (200 g/L) was fed by means of a tubular pump and together with air flow was adjusted in order to have the desired pH value (> 6) in the reactor. The pH and redox potential were continuously monitored.

2.2.2 Solvent extraction

The experimental arrangements of manganese solvent extraction are shown in detail elsewhere (Article II), but the principles of the methods are briefly described here. The extraction isotherms of metals for D2EHPA and CYANEX 272 were determined at different temperature by equilibrium experiments in a jacketed 1 L glass reactor. Different phase ratios were used. The solution pH was adjusted with aqueous ammonia or concentrated H_2SO_4 . The solution pH was measured using a calibrated glass calomel electrode. The mass balance was checked by analyzing samples taken from both phases. The mixing time in every experiment was 15 minutes before sampling or phase separation. The extraction equilibrium was also verified by a constant pH reading according to the Eq. 20.

Several extraction diagrams as a function of Mn concentration (McCabe-Thiele diagrams) were determined at solution pH 3.0, 3.5, 4.0, 4.5, and 5.0. The idea of the McCabe-Thiele diagrams were to study the effect of concentration on metal extraction on organic extractant. By these diagrams the amount of extraction steps required to recover manganese with chosen phase ratio and pH was able to be seen. Experiments were carried out by mixing synthetic metal solution with varying metal concentration and organic extractant at known phase ratio and at the chosen temperature.

Counter current SX process

A counter-current manganese extraction process was simulated by batch wise experiments with an authentic metal solution at 40°C. 25 vol-% phosphinic acid (diluted with an aliphatic diluents, Exxsol D-80) was chosen for extractant since it is more selective to manganese against calcium than phosphorus acid extractant. In addition the possibility to operate at higher temperature with CYANEX 272 is closer the optimum in the view of solution viscosity. The effect of pH on the three-step manganese extraction was studied by equilibrating authentic multi-metal solution with pre-loaded or with fresh 25 vol-% extractant in H-form at different pH. The metal raffinate solution from the first step was removed to the second extraction step and in the third step the metal raffinate from the second step was equilibrated with fresh extractant at the lowest pH. Two parallel experiments were made, in which only the equilibrium pH was changed.

In addition to extraction, two different scrubbing solutions for impurity removal from the organic phase was investigated. The scrubbing was carried out in two steps by using loaded

extractant and pure DI water or 1 mmol/L H₂SO₄ solution. Finally the scrubbed extractant was stripped in two steps using H₂SO₄ solution in high phase ratio (O/A >10).

2.2.3 Ion Exchange

Equilibrium, kinetic and dynamic column experiments were done with synthesized manganese oxide materials, called also as Octahedral Molecular Sieve (OMS) in order to elucidate their ion exchange properties in heavy metal removal from hydrometallurgical and natural solutions. Proton and metal ion binding properties of dry and finely ground OMS materials were titrated in a constant supporting electrolyte (NaNO₃) concentration ($I = 0.1$ mol/L) at room temperature (25°C). Metal titrations were carried out with the same method by replacing a constant amount (0.1 mL) of NaNO₃ solution with 0.1 M Me(NO₃)₂ solution (Me = Cu or Ni). The total volume of a single batch was 10 mL. The exact amount of each reagent was calculated from the weighed masses and the measured densities. The proton concentration was obtained from the pH measurement by calibrating the pH electrode against known amounts of acid and base at the same ionic strength used in the titration. The more detailed descriptions of the manganese oxide synthesis, support on silica and metal adsorption on the final product are reported in the Articles III - VI.

2.3 Modeling

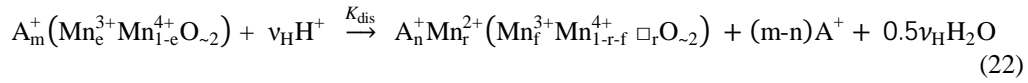
The properties of the synthesized OMS materials as ion exchanger were studied and modeled in specific experiments. Detailed descriptions of the used models are presented in the Articles IV and VI, but the main idea is also shown here. Metal loading from the solution to the solid phase is assumed to follow either an ion exchange or redox mechanism. Ion exchange takes place at the negatively charged sites present in the OMS structure. The ion-exchange equilibrium is described using a non-ideal competitive adsorption (NICA) model (Sirola *et al.*, 2008). The specifically bound amounts, q_s , of protons and metal cations can be calculated from Eq. (21), where κ and c are the affinity constant and the molar solution concentration. The parameter h depends on the binding stoichiometry and on the lateral interactions of the adsorbed species. The heterogeneity of the sites is characterized by the value p ($0 < p \leq 1$).

$$q_{sp,i} = q_{max} \left(\frac{h_i}{h_H} \right) \frac{(\kappa_i c_i)^{h_i} \left[\sum_j (\kappa_j c_j)^{h_j} \right]^{p-1}}{1 + \left[\sum_j (\kappa_j c_j)^{h_j} \right]^p} \quad (i, j = H, Me) \quad (21)$$

It is assumed here that the maximum proton binding capacity is equal to the total amount of sites, q_{max} . The total bound amount of cation i is then $q_i = q_{sp,i} + q_{b,i}$. Invasion of anions in the nanopores is considered negligible at the studied conditions. In addition to ion exchange mechanism, metal ions can adsorb on the manganese oxide framework by redox mechanism since at low pH Mn⁴⁺ tend to reduce to Mn³⁺. Mn³⁺ may also disproportionate further according to $2Mn^{3+} \rightleftharpoons Mn^{2+} + Mn^{4+}$. This process can be formally expressed by means of Eq. (22). A vacancy (\square) is also created when Mn²⁺ moves from the framework to interstitial sites and becomes exchangeable. Excessively acidic conditions were avoided and therefore, this effect was not included in the model. The NICA parameters were estimated from the titration and

sorption equilibrium data by trial-and-error. Consequently, the parameters are useful for correlation only, and comparison of individual values is difficult. The differential and arithmetic equations were solved numerically as described by Sirola *et al.*, (2008). The number of axial grid points was 60 and the time step was typically 1-5 s. Further increase in the number of the grid points did not affect the results.

Ion exchange is assumed to be the only mechanism for binding of cations other than manganese. As described in Articles IV and VI, changes in the manganese oxide framework at low pH values must also be considered.



Here K_{dis} is the apparent equilibrium constant. It is assumed that only a certain fraction of Mn^{3+} undergoes disproportionation and the above-mentioned stoichiometry gives $r = 0.5(e-f)$. A^+ represents an exchangeable univalent counter-ion and ν_H is considered as an adjustable parameter.

Batch Operation

The transport of ions in the layered or tunnel-type manganese oxide micro-crystals was described using the Nernst-Planck equation. No distinction was made between specifically and non-specifically bound species and only the overall values, q , were used for solid concentrations. One-dimensional diffusion is assumed for both structures. In a system of N mobile ions, the flux of ion i , J_i , can thus be given by Eq. (23) (Carta and Lewus, 1999).

In order to simplify calculations, the solid phase accumulation term was evaluated using the approximate solution (Carta and Lewus, 1999). In the approximate approach, the concentration profiles within the oxide particles are not calculated but the driving force is evaluated approximately from the difference between the surface and average concentrations. The approximate expression for the flux of ion i becomes as follows.

$$J \approx -\frac{2z_i D_{s,i}}{\rho_s d(L)} \frac{\left[\bar{q}_i - q_i^* \exp\left(\frac{z_i m}{5}\right) \right]}{1 - \exp\left(\frac{z_i m}{5}\right)} m \quad (23)$$

D_s is the micro-crystalline diffusion coefficient, ρ_s is the material density, z is the ion charge, and the parameter m is obtained from the condition of zero net current (Carta and Lewus, 1999). The symbols with an over-bar and an asterisk represent the average and surface values, respectively. Assuming that external mass transfer resistance is negligible and local equilibrium is established at the particle surface, q_i^* is related to the solution concentration by Eq. (21). The mass balances for the two particle geometries are shown in Eq. (24).

$$\frac{\partial \bar{q}_i}{\partial t} = -\frac{1}{\rho_s} \left(\frac{4}{d} J_i - \nu_i r_{dis} \right) \quad (OL-1)$$

$$\frac{\partial c_i}{\partial t} = \frac{4V_s}{V_{\text{liq}}d} J_i$$

(24)

$$\frac{\partial \bar{q}_i}{\partial t} = -\frac{1}{\rho_s} \left(\frac{2}{L} J_i - v_i r_{\text{dis}} \right) \quad (\text{OMS-1 and OMS-2})$$

$$\frac{\partial c_i}{\partial t} = \frac{2V_s}{V_{\text{liq}}L} J_i$$

$$r_{\text{dis}} = k_{\text{dis}} \left[q_{\text{Mn}^{3+}}^\alpha q_{\text{H}^+}^\beta (q^\theta)^{-(\alpha+\beta)} - \frac{1}{K_{\text{dis}}} q_{\text{Mn}^{2+}}^\gamma (q^\theta)^{-\gamma} \right]$$

$$K_{\text{dis}} = \frac{q_{\text{Mn}^{2+}}}{q_{\text{Mn}^{3+}}^2 q_{\text{H}^+}^{\nu_{\text{H}}}} (q^\theta)^{\nu_{\text{H}}+1}$$

The disproportionation of Mn^{3+} (Eq. 22) is accounted for by a simplified solid-phase reaction with a rate constant k_{dis} and an apparent equilibrium constant K_{dis} . The orders were assumed equal to the stoichiometric coefficients; $\alpha = 2$, $\beta = \nu_{\text{H}}$ and $\gamma = 1$. The unit concentration (1 mol/kg) is represented by q^θ . It was assumed on the basis of acid uptake measurements that mass transport in the silica composites is controlled by diffusion in the OMS crystals. The same equations were thus used to obtain apparent diffusion coefficients for the supported crystals.

Fixed-Bed Operation

The overall mass balance for the fixed-bed system is given by Eq. (25). An axially dispersed flow through the bed is assumed and D_{ax} is the dispersion coefficient. Interstitial flow velocity is represented by u and x is the axial coordinate. The volume fraction of the OMS crystals is given by η and $\varepsilon_{\text{tot}} = 1 - (1 - \varepsilon_p)(1 - \varepsilon_b)$ is the total bed porosity, where ε_b is the bed porosity and ε_p is the pore volume fraction of the silica composite.

$$\frac{\partial c_i}{\partial t} + \frac{\rho_s \eta}{\varepsilon_{\text{tot}}} \frac{\partial q_i}{\partial t} = -u \frac{\partial c_i}{\partial x} + D_{\text{ax}} \frac{\partial^2 c_i}{\partial x^2}$$

(25)

The initial and boundary conditions were as follows, where c^{init} and c_{feed} refer to the initial and feed concentrations in the batch and fixed-bed experiments, respectively.

Batch:

$$t = 0: \quad c_i = c_i^{\text{init}}, \quad q_i = 0$$

$$t > 0, \quad y = 0: \quad \frac{\partial q_i}{\partial y} = 0$$

Fixed bed:

$$t = 0: \quad c_i = c_i^{\text{init}}, \quad q_i = q_i^{\text{init}}$$

$$t > 0, \quad x = 0: \quad \frac{\partial c_i}{\partial x} = -\frac{u}{D_{\text{ax}}} (c_{\text{feed},i} - c_i)$$

The axial dispersion coefficient was estimated from known correlations as $5 \cdot 10^{-7} \text{ m}^2/\text{s}$. A value of 0.4 was used for the bed porosity ε_b . The density of the OMS crystals is taken as 3 g/mL. In all calculations, the changes in the OMS mass were neglected. Highest acid concentration was used in column experiments and even there the amount of Mn removed constituted only 2% of the total OMS mass.

2.3 Synthesis of OMS materials

Detailed description of the synthesis of OMS materials and making of silica-supported compounds are shown in Articles III - VI but short discussion is given also here. Na-buserite was synthesized by mixing a MnSO_4 solution ($c_{\text{Mn}} = 0.6 \text{ mol/L}$) slowly added (ca. 4 mL/min) 5M NaOH solution under N_2 atmosphere and under vigorous mixing (600 1/min with a Teflon coated impeller). The temperature was kept below 10°C by an ice water bath. After precipitation, Mn was oxidized by feeding 1.5 L/min of oxygen (AGA, Finland) in the reactor. The duration of each run was 24 h. Finally, the solid was filtered and washed with deionized water until pH was between 9 and 10. Na-buserite was used as the starting material for Mg-todorokite (OMS-1). Washed and centrifuged Na-buserite were first converted to Mg-buserite by MgCl solution ($c_{\text{Mg}} = 1 \text{ mol/L}$) for 24 h under reflux. After refluxing, the solid was washed with deionized water and centrifuged.

K-cryptomelane (OMS-2) material was synthesized according to DeGuzman *et al.*, (1994) using the hydrometallurgical raffinate simulant. 0.15M Na_2SO_4 was used as a base solution in which the other metal sulfates were dissolved. The volume of the mixture was increased to 500 ml using deionised water and 11.5 ml of 65% HNO_3 was poured to the mixture. 2.1 g of KMnO_4 was added and the mixture was heated to its boiling point and refluxed for 24 h. A magnetic stirrer was used throughout the synthesis. Finally, the precipitate was separated and washed with DI water until the effluent was free of acid and the solids were dried at 120°C .

Binding of OMS with silica

The binding of OMS materials on silica is detailed described in Article V. A short description is also shown here. Washed and air-dried (moisture content about 70%) OMS material was added into colloidal silica solution (Ludox LS40, Grace Davison) adjusted to pH 4 with 2M HCl. The mixture was homogenized both by a mechanical stirrer and ultrasonication. OMS material and silica were mixed in a dry weight ratio of 2/3. The mixture was first solidified at 110°C for one hour, crushed and then heated again at 110°C for another hour. Finally the hard materials were gently ground in a mortar and sieved to the particle size range 125 - 400 μm . Finally, the composites were heated in air at 250°C for two hours.

2.4 Analysis

Detailed description of analysis method are shown in Articles I-VI. The meaning of different analysis for the studies are discussed here.

2.4.1 Titrations

The capacity (amount of functional group) of extractant (solid ion exchanger) were determined by titration with known acid or base solutions. In addition, acid-base titration is useful method to characterize the acid-base properties (relative acidity) of the separation material and evaluate its

suitability for the separation. For the evaluation of the synthesized OMS materials, the average oxidation state of manganese was determined by redox titration described in Article VI.

2.5.2 Spectroscopic and chromatographic methods

The concentration of metal ions in solution was analyzed in order to evaluate the properties of used precipitation method or characterizing the ion exchange properties of extractant, or solid ion exchanger. The change in metal ion concentration between the samples taken in time scale or reagent addition scale gives knowledge for the reaction kinetics and mechanism and show the stoichiometry. Also the extraction capacity and selectivity of extractant for metals could be calculated based on the spectroscopic analysis of metal ions. Inductive Coupled Plasma - Atomic Emission Spectrometer (Iris Intrepid II XDL ICP-AES) was used in order to analyze simultaneously several elements. The precision of the method used is generally high ($c_1 < 1$ mg/L). In some cases, however, the small concentrations (≈ 1 mg/L) of metals in the highly concentrated Mn and NH_4 sulfate solutions were not possible to be analyzed reliably. The metals from the organic solutions were stripped with known amounts of 2 M H_2SO_4 at an O/A volume phase ratio of 1/20 before analysis. Experimental accuracy was controlled by calculating the mass balance for the metals in both phases.

NH_4^+ ions were analyzed by electrophoresis (P/ACETM MDQ Capillary Electrophoresis System by Beckman Coulter). Separation of the ions was done with a silicon capillary (Polymicro Technologies TSP050375) of length 0.1 m. The injection time was 15 seconds at a pressure of 6.9 kPa. The ion acceleration voltage was 30 kV. Some reference measurements for ammonium sulfate were done with a thermal analyzer (Netzsch STA 449 C Jupiter) connected to a quadrupole mass spectrometer (Netzsch QMS 403 Aëolos[®]). The ammonia nitrogen was detected by heating (burning) samples in an O_2 atmosphere at the rate of $10^\circ\text{C}/\text{min}$ and analyzing the evaporated NO_x compounds. The same apparatus was used in determining of moisture content of solid materials, respectively.

2.4.3 Physical characterization

Characterization of used extractant and synthesized OMS material required several different analysis and measurements. In order to clarify the effect of temperature on solvent extraction the viscosity measurements need to be made. The density of metal solutions and reagents were determined in order to use the mass of reagent instead of volume, which is more complicated to measure exactly. With surface area (BET) and particle size measurements, some duplicate samples were made.

The structural analysis of materials were made using spectroscopic methods, scanning electron microscopy (SEM) with JEOL JSM-5800 microscope equipped with an ultra dry X-ray detector from Thermo Fisher Scientific Inc, N_2 adsorption (BET) measurements with Micromeritics Gemini V, and particle size measurements with Coulter LS130. Crystal structure and purity was verified by means of X-ray powder diffractometry (XRD, PANAnalytical X'pert PRO and Phillips PW 1710 powder diffractometer with Cu K_α (0.154 nm) radiation). IR spectra were obtained using the standard KBr tablet method on a Perkin-Elmer 2000 FT-IR spectrometer.

3. RESULTS AND DISCUSSION

The aim of this work was to study the appropriate methods including precipitation, solvent extraction and ion exchange, for manganese recovery and refining from multi-metal tailings. In the first step, manganese was separated from iron using chemical precipitation (Article I). After iron removal, the effect of temperature on Mn selectivity over Ca and Mg with two commercially available phosphorus acid extractants was studied (Article II). Finally the syntheses of Octahedral Molecule Sieve materials (OMS) and their support on silica were done (Articles IV - VI). The properties of synthesized materials and their characters in ion exchange applications were elucidated.

3.1 Precipitation of manganese and iron

Experimental arrangements and the results of manganese and iron precipitation studies are shown in Article I. Due to the wide occurrence of iron in hydrometallurgical solutions and its properties, iron typically decreases the technical and economical efficiency of metals separation. The calculations (HSC Chemistry[®] 6.1) for Eh-pH diagram of Mn-Fe-S system show that in theory iron is possible to be separated from manganese, when the pH and redox potential have specific values (Fig. 4). Iron is possible to be separated from soluble manganese sulfate as metallic or as iron sulfide at pH from 0 to 8.5, when redox potential is below -0.5 V or as FeO·OH when pH is between 1 and 7.5 and redox potential between 1.2 and -0.2 (a waved area in Fig. 4). Using oxidative or reductive methods, iron and manganese precipitation with different reagents were studied in order to find optimal conditions for the production of a MnSO₄ solution free from iron.

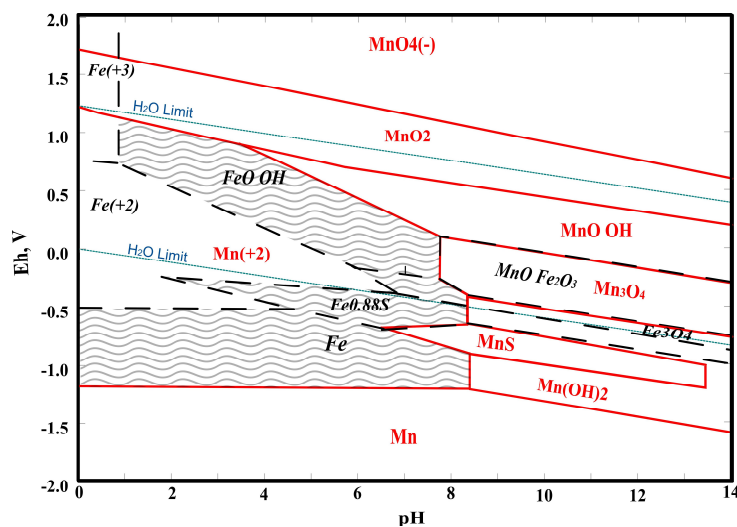


Figure 4. Calculated Eh-pH diagram for manganese (solid lines) and iron (dashed lines) compounds in a Mn-Fe-S system at 25°C. A waved area correspond the conditions, where iron is in solid form and separates from soluble manganese. Calculations were done with HSC Chemistry[®] 6.1 software.

The carbonate ion (CO_3^{2-}) is quite passive and do not involve in redox reactions (measured redox potentials in Figs. 5B and 6B). This makes it possible to compare carbonate and hydroxide precipitation and formation of solid precipitates. NaHCO_3 , Na_2CO_3 , and CaCO_3 slurries (2.38, 1.89, and 2.0 mol/L) were used and studied as carbonate sources for metal precipitation. The effect of oxidation on precipitation was studied by feeding 3.6 mmol/min O_2 or using 9.3 mmol MnO_2 . The initial volume of the experiments was 0.5 L. The metal concentrations, the calculated, and measured redox potential values during the experiment are shown in Fig 5B. The effect of reagent feed rate on the properties of precipitates is shown in Table 3.

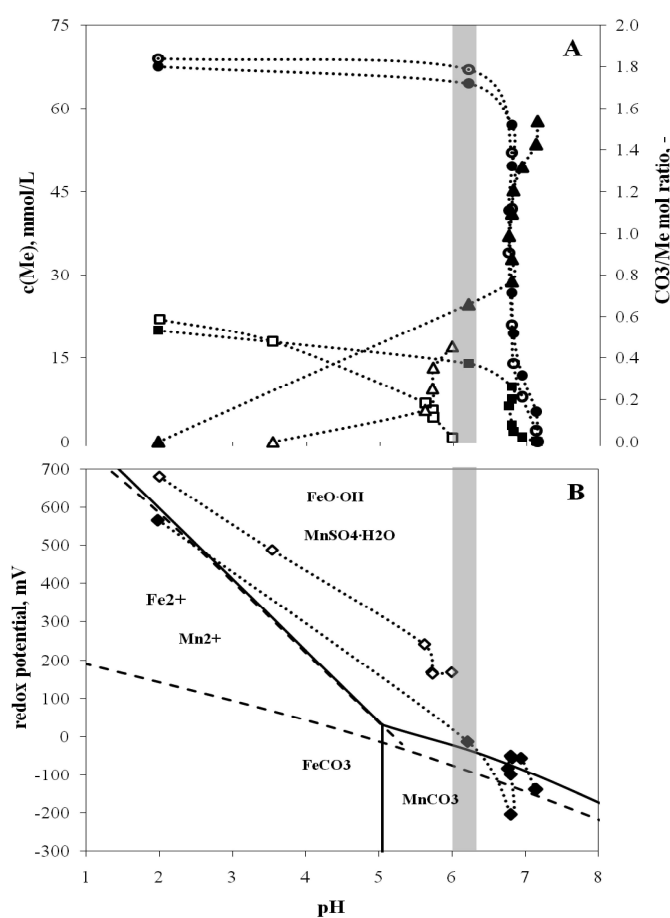


Figure 5. Manganese and iron precipitation with carbonate. Experimental metal concentrations in solution in the presence of O_2 (open symbols) and without O_2 (filled symbols) (A) and the corresponding redox potentials in SHE scale (B). $T = 40^\circ\text{C}$. The symbols are Mn (●, ○), Fe (■, □), and CO_3^{2-} (▲, △), and redox potential (◆, ◇). Solid lines for Mn and dashed lines for Fe are calculated with HSC Software.

A window for optimal precipitation condition can be seen in Fig.5, indicated by a shaded area. Selective separation of iron from manganese with CaCO_3 can be done in the presence of O_2 at pH from 5.9 to 6.2 (in fig.5A). Simultaneous addition of CaCO_3 and O_2 is an effective method to remove iron from solution avoiding manganese co-precipitation. Under these conditions, iron is in solid phase ($\text{FeO}\cdot\text{OH}$) and manganese in liquid (Mn^{2+}). Iron precipitation is complete at pH 6.0 and at redox potential > 200 mV. The CaCO_3/Fe ratio follows the stoichiometry fairly well. It can be concluded that in order to get full iron precipitation, the O_2/Fe and CaCO_3/Fe mole ratios should be at least 4 and 1.1, respectively. The amount of O_2 was four times the stoichiometric need, which was most likely due to inefficient mixing. An alternative explanation for high O_2 consumption would be more complicated; a mechanism based on the formation of peroxy dicarbonate similar to the proposed by Zhang *et al.* (2000a) for iron oxidation with sulfite and peroxy monosulfate radicals. The oxygen feed also seemed to have a great effect on solution pH; a finding which is assumed to be a result of interaction between O_2 and H^+ . Good mixing was observed to be essential for effective gas dispersion and optimum mass transfer.

There is no selectivity window for iron and manganese with CO_3^{2-} when no oxidation is used, since they precipitate together at $\text{pH} \approx 7$. Comparison of measured redox potential (from 0 to -200 mV) to the calculated Pourbaix diagrams indicates iron precipitating as ferric oxo hydroxide (Eq. 13). Formation of FeCO_3 is not possible since the value of redox potential is too high. Due to the low initial pH (2.1), about 40% of used CO_3^{2-} ions were consumed in acid neutralizing (rising pH up to 6). Redox potential of the system decreased until the metals were fully precipitated (Fig. 5B, $\text{pH} = 7.1$ and redox potential - 140 mV). No effect of the feed rate of NaHCO_3 or Na_2CO_3 on the metal precipitation was observed when the shift was from 1.3 to 1.7 mmol/min (Table 3). The parallel experiments with solid reagents, however, showed that during slow addition (< 2 mmol/min) of reagent and long lasting experiment (60 min), iron precipitated more effectively. This was due to the oxidation reaction of Fe^{2+} to Fe^{3+} (Eq. 12), which is, however, very slow at pH under 3 (Zhang, 2000a), (Zhang *et al.*, 2000b). Comparison between NaHCO_3 and Na_2CO_3 showed that only the final oxidation potential was slightly lower with Na_2CO_3 (about 150 mV) resulting iron to precipitate partly as FeCO_3 and ferric oxo hydroxide. Due to the lower potential, iron precipitation was inhibited and iron precipitated together with manganese as mixed solid (90% of Mn was precipitated at the point where Fe was fully precipitated). Total consumption of reagent (in moles) was only a half of that used in previous experiment with oxidation.

Hydroxide precipitation of metals from the authentic solution using $\text{Ca}(\text{OH})_2$ slurry (2.7 mol/L) are shown in Fig. 6. The initial volume of both experiments was 0.5 L. The calculated and measured redox potential values during the experiment are also shown (Fig. 6B).

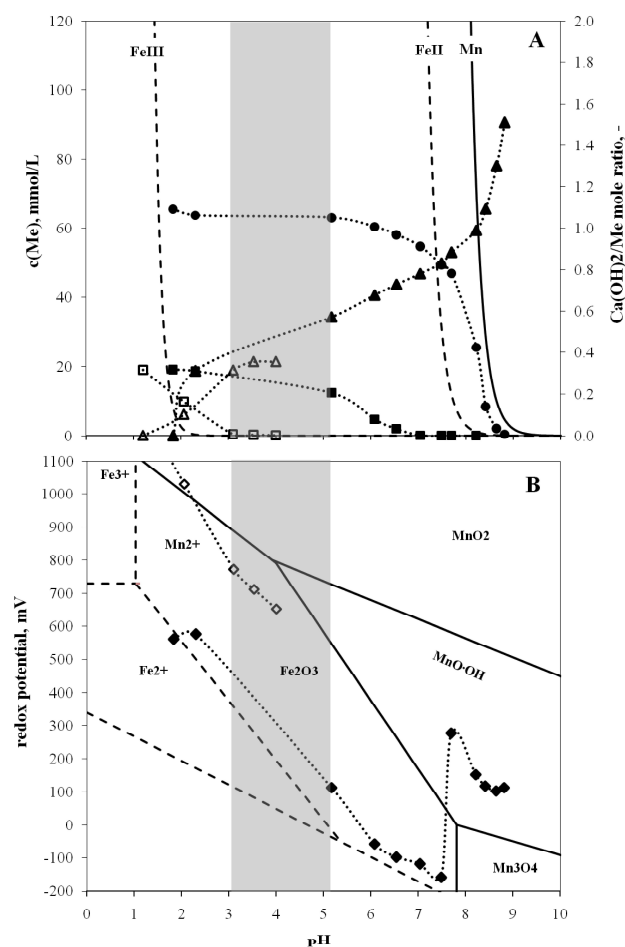


Figure 6. Manganese and iron precipitation with hydroxide. Experimental metal concentrations in solution in the presence of MnO_2 (open symbols) and without MnO_2 (filled symbols) (A) and the corresponding redox potentials in SHE scale (B). $T = 40^\circ\text{C}$. The symbols are Mn (\bullet), Fe (\blacksquare , \square), $\text{Ca}(\text{OH})_2/\text{Me}$ mol ratio (\blacktriangle , \triangle), and measured redox potential (\blacklozenge , \diamond). Solid lines for Mn and dashed lines for Fe are calculated with Eq.14 (A) and HSC Software (B).

Iron precipitation as hydroxide is similar to the precipitation as carbonate. A window for optimal precipitation conditions, indicated with a shaded area, can be seen in Fig. 6. The addition of MnO_2 increased the initial redox potential above 1000 mV, which effectively oxidized Fe^{2+} to Fe^{3+} . with $\text{Ca}(\text{OH})_2$, the oxidized iron was selectively precipitated already at about pH 3 (Fig. 6A). The oxidation potential of the system was high (from 650 to 800 mV) and iron was assumed to precipitate as hematite Fe_2O_3 having good filtration properties (Table 3). The consumption of the reagent (0.27 mmol) followed well the stoichiometry of Eq. 13. If no iron oxidation is used, only low precipitation occurs at pH below 5. Further increase in pH also increases iron oxidation and total precipitation is reached at pH above 7. Sulfide precipitation of iron and manganese is shown in Fig. 7.

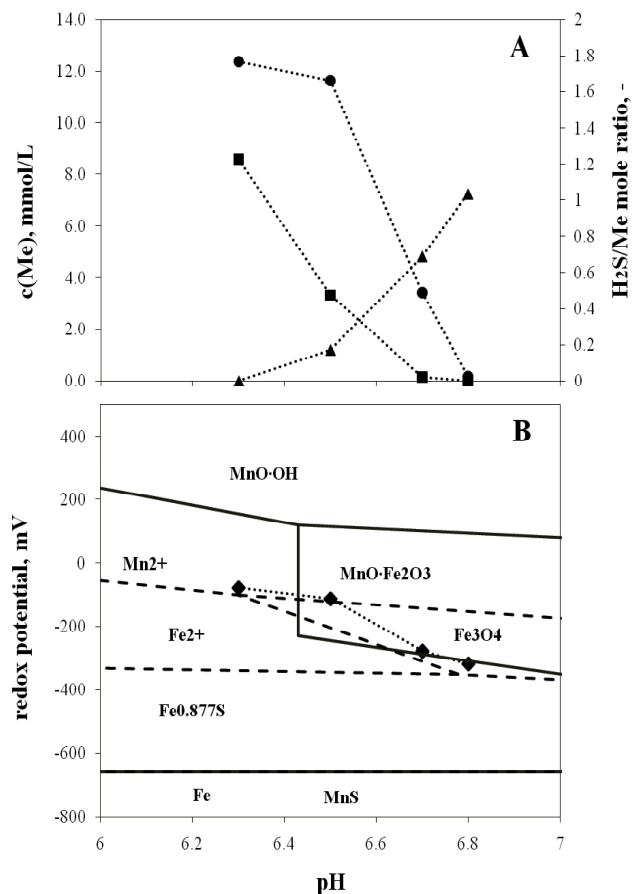


Figure 7. Manganese and iron precipitation with sulfide. Experimental metal concentrations in solution (A) and the corresponding redox potential values (B). $T = 70\text{ }^\circ\text{C}$. Symbols Mn (●), Fe (■), $\text{H}_2\text{S}/\text{Me}$ mole ratio (▲), and measured redox potential (◆). Solid lines for Mn and dashed lines for Fe are calculated with HSC Software.

With sulfide, no window for selective separation was found. Manganese and iron precipitated simultaneously with sulfide precipitation (Fig.7A). The measured redox potentials showed too high values for the formation of pure single metal sulfides. According to the calculations with HSC, the mixed precipitates were formed, which is the reason for the simultaneous precipitation. Comparison between the solubility products of individual metal sulfides ($\text{p}K_{\text{sp}} = 12.6$ for Mn^{2+} and 17.2 for Fe^{2+}) (Dean, 1999) suggest better separation selectivity. According to Wei and Osseo-Asare, (1996), solution Eh-pH has a significant role in the formation of iron precipitate in meta-stable Fe-S- H_2O system. Furthermore, a long aging time (several days) is needed for pyrite (FeS_2) formation.

The oxidative precipitation of iron and manganese from the authentic solution using SO_2/O_2 gas mixture with 1M NaOH solution is shown in Figure 8. The experiment was done at 40°C in a glass reactor with a volume of 0.5 L. The calculated and measured redox potential values during the experiment are also shown. The properties of precipitates from parallel experiments with different reagent feed rate are shown in Table 3.

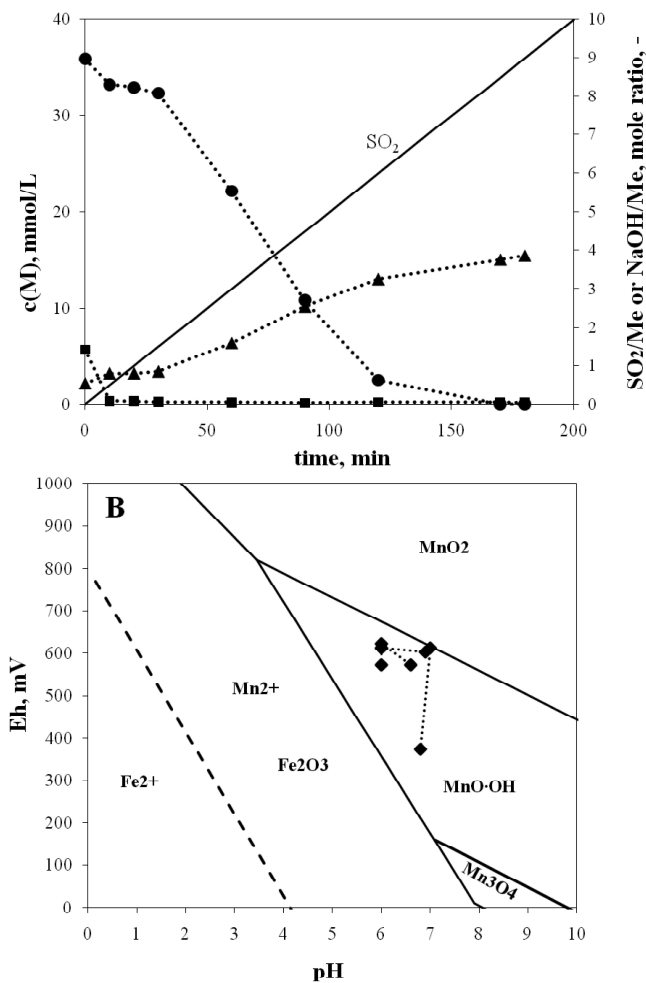


Figure 8. Manganese and iron precipitation with SO_2/O_2 . Experimental metal concentrations in solution on time scale (A) and the corresponding redox potential values on pH scale (B). The symbols are Mn (\bullet), Fe (\blacksquare), the measured redox potential (\blacklozenge), and NaOH/Me (\blacktriangle). SO_2 feed was 2.5 mL/min and $T = 40^\circ\text{C}$. Solid lines for Mn and dashed lines for Fe are calculated with HSC Software.

The oxidation and precipitation of iron with O₂/SO₂ gas mixture is very effective and selective for manganese over several metals. Precise gas feed control is essential due to the complicated reaction mechanisms between O₂ and SO₂, and the sensitive dependence of the redox potential on these mechanisms (Zhang *et al.*, 2002). Depending on pH and the O₂/SO₂ ratio, MnO·OH, Mn₂O₃, or MnO₂ may be formed. The consumption of NaOH (1 mol/L) during precipitation varied from 2.9 to 4 mol NaOH/1 mol Mn, with an average value of 3.6. Comparison of the measured redox potential with the calculated phase diagram (Fig. 8B) confirms the formation of mixed oxide.

Table 3 Effect of precipitation parameters on solid properties.

reagent	Oxidizer	Reagent feed rate, mmol/min	Settling rate, cm/min	Filtration capacity (dry solid), kg/m ² h
NaHCO ₃	-	1.3	4.0	3.7
NaHCO ₃	-	1.7	0.0	3.6
Na ₂ CO ₃	-	0.5	3.0	25.0
Na ₂ CO ₃	-	1.1	1.8	23.0
Na ₂ CO ₃	-	1.5	2.7	23.0
Na ₂ CO ₃	-	2.5	1.5	29.0
Na ₂ CO ₃	-	3.5	1.0	30.0
Na ₂ CO ₃	-	10	1.1	72.0
Ca(OH) ₂	-	1.3	3.9	49.0
Ca(OH) ₂	-	2.0	1.4	149.0
Ca(OH) ₂	-	2.7	0.3	99.3
Ca(OH) ₂	MnO ₂	0.8	0.0	49.0
Ca(OH) ₂	MnO ₂	2.2	0.0	163.0
CaCO ₃	O ₂	0.2	3.2	86.0
CaCO ₃	O ₂	0.4	9.4	36.9
CaCO ₃	O ₂	0.5	3.0	71.9
CaCO ₃	MnO ₂	2.0	0.0	13.4
H ₂ S	-	3.1	-	60
SO ₂ /O ₂	SO ₂ /O ₂	36 (tot)	5	80

The settling properties of the solids were very dependent on the reagent feed rate. However, with Na₂CO₃ and CaCO₃, the variation was rather large. It can be concluded that in addition to the super-saturated state, nucleation and crystal growth depend also on other parameters. In some experiments, the precipitate did not easily settle and could not be filtered without the use of flocculants (reported also by Claassen *et al.*, 2002). With slow feed rates, good settling properties were found for all reagents except H₂S. The sulfide particles were too fine-grained to be able to ascertain a reliable value for settling. Filtration properties were not as sensitive to feed rate, and no clear connection can be seen between filtration and feed rate. The biggest values (163 and 149 kg/m² h) were found with hydroxide precipitation. The moisture content of the hydroxide precipitates was, however, significantly higher; 70 - 85% for hydroxide precipitates and 55 - 70% for other precipitates. Moreover, formation of gypsum with Ca-containing chemicals significantly changed the amount of solids and their properties.

3.2 Acid leaching of manganese concentrate

The leaching properties of the manganese precipitates were studied in order to compare the precipitation methods and to optimize the acid consumption. Comparison is made since the recovery of manganese from multi-metal solution with low concentration is economical only with the most chemical and energy efficient methods. Leaching is needed in cases, where precipitation is applied to make a solid Mn intermediate. Carbonate and hydroxide reagents were compared in terms of leaching selectivity and acid consumption (Table 4).

Table 4 The effect of acid to Mn ratio (mole) on the leaching of Mn and Fe from the different precipitates.

precipitant	H ₂ SO ₄ / Mn ratio, -	Mn leached, (%)	Fe leached, (%)
Ca(OH) ₂	1.5	50	67
Ca(OH) ₂	3.0	47	77
Ca(OH) ₂	5.8	42	75
Na ₂ CO ₃	0.7	63	-
Na ₂ CO ₃	1.2	86	14
Na ₂ CO ₃	1.3	91	22
Na ₂ CO ₃	1.6	93	79
Na ₂ CO ₃	2.6	97	84

The results clearly show that acid consumption in leaching with carbonate precipitation is significantly smaller than with hydroxide precipitate. Iron was leached similarly from both precipitates with the same acid ratio. This finding also confirms iron to be precipitated with the same mechanism as FeO-OH independently of the precipitant. Moreover, the parallel experiments with varying acid concentration (from 0.5 to 2 mol/L) showed that the total acid amount is more significant for leaching efficiency than acid concentration (Eqs. 9 and 10).

3.3 Separation of manganese by solvent extraction

According to Article II, manganese solvent extraction and selective separation from Ca and Mg can be done with organophosphorus acid extractants. The temperature has, however, a significant effect on the extraction equilibrium and selectivity.

Effect of pH and temperature on extraction isotherms

The extraction equilibria of metals with di-(2-ethylhexyl) phosphoric acid (D2EHPA) and bis-(2,4,4-trimethylpentyl) phosphinic acid (the active compound in CYANEX 272) are shown in Figures 9 and 10. Extraction of metals as a function of solution pH was determined with multi-metal solutions at different temperatures.

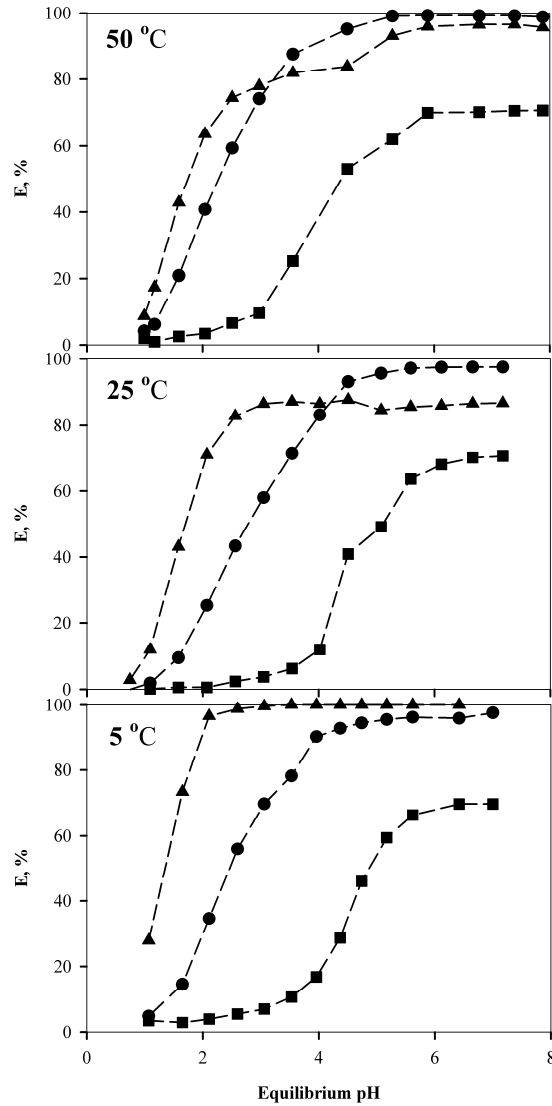


Figure 9. Extraction isotherms for 25 vol-% D2EHPA at three temperatures. $I_c = 0.9$ M, $[Ca]_0 = 6$ mmol/L, $[Mn]_0$, $[Mg]_0$, $[Na]_0 = 100$ and $[SO_4^{2-}]_{tot} = 250$ mmol/L. Symbols: Mn (●), Mg (■), Ca (▲).

The temperature has a significant effect on metal extraction with D2EHPA. The pH_{50} value for Ca decreased from 1.67 to 1.32 as the temperature decreased from 50 to 5°C. At the same temperature range, the pH_{50} value of Mn changed by 0.3 units (from 2.24 to 2.54). These values are consistent with the observations of (Cheng, 2000) for Mn and Ca at temperatures of 23 and 60°C. The ΔpH_{50} values of Ca and Mn are shown in Table 5. Interestingly, the shift of isotherms for Mn and Mg was biggest at the temperature change from 50 to 25°C and further temperature

decrease caused only a slight further shift. Calcium behaved differently. The change in temperature from 50 to 25°C had practically no effect on the pH_{50} value, but a remarkable change could be observed at 5°C.

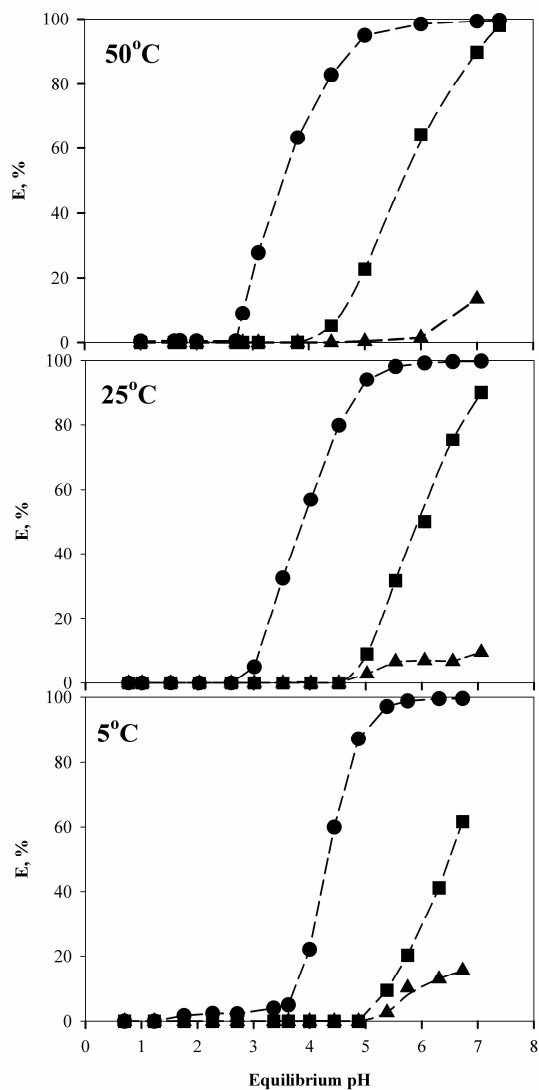


Figure 10. Extraction isotherms for 25 vol-% CYANEX 272 at three temperatures. $I_c = 0.9$ M, $[\text{Ca}]_0 = 9$ mmol/L, $[\text{Mn}]_0 = 110$, $[\text{Mg}]_0 = 80$, $[\text{Na}]_0 = 110$ and $[\text{SO}_4^{2-}]_{\text{tot}} = 250$ mmol/L. Symbols: Mn (●), Mg (■), Ca (▲).

Table 5 Calculated ΔpH_{50} values and selectivity coefficients ($K_{\text{Mn}/\text{Ca}}$) for metals at different temperatures. Selectivity coefficients for D2EHPA were calculated at pH 2.5 and those for CYANEX 272 at pH 5.0.

	D2EHPA			CYANEX 272		
	5°C	25°C	50°C	5°C	25°C	50°C
$\Delta\text{pH}_{50} \text{ Mn/Ca}$	1.22	1.08	0.57	a	a	a
$\Delta\text{pH}_{50} \text{ Mn/Mg}$	2.05	2.03	2.05	2.10	1.95	2.05
$K_{\text{Mn}/\text{Ca}}$	$1.5 \cdot 10^{-3}$	$1.9 \cdot 10^{-2}$	0.15	$>10^7$	$>2 \cdot 10^6$	$>10^5$
$K_{\text{Mn}/\text{Mg}}$	480	540	470	5100	4300	550

a: Could not be calculated

In the case of CYANEX 272 the effect of temperature on the manganese pH isotherm was similar to that of D2EHPA. The ΔpH_{50} value of manganese was 0.49 (from 3.83 to 4.32) when the temperature was changed from 25 to 5°C. At the same temperature range the pH_{50} value of Mg changed by 0.18 pH units (from 5.95 to 6.13). The pH_{50} value for Ca could not be calculated due to low extraction (under 50%). Comparison of the pH isotherms of D2EHPA and CYANEX 272 (Figs. 9 and 10) and the calculated selectivity coefficients clearly show that CYANEX 272 is a much better choice for selective Mn separation from solutions rich in Ca. The difference in Mn-Mg separation is not as clear, however, although CYANEX 272 seems to show slightly better performance.

Calcium can be extracted prior to manganese with D2EHPA, but the difference in ΔpH_{50} values between Ca and Mn, even at 5°C, was not enough to make the extraction selective ($K_{\text{Ca}/\text{Mn}} \approx 670$). Approximately 30 - 50% of manganese would be lost as co-extraction. These results clearly show CYANEX 272 to be a feasible choice for manufacturing pure MnSO_4 , which can be used as starting material for the production of metallic manganese, manganese dioxide (CMD or EMD) (Nijjer, 2000) or pure manganese chemicals.

McCabe-Thiele diagrams

The effect of concentration on manganese extraction at pH 4 and 4.5 with 25 vol-% CYANEX 272 diluted with Exxsol D80 by McCabe-Thiele diagrams are shown in the figures 11 and 12.

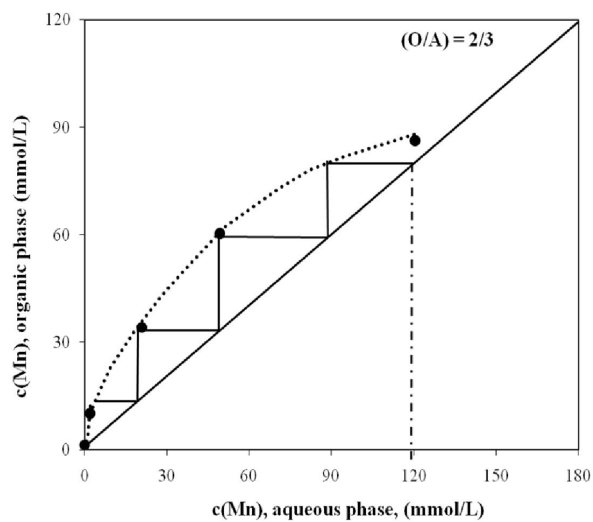


Figure 11. The effect of concentration on manganese extraction on 25 vol-% bis-(2,4,4-trimethylpentyl) phosphinic acid reagent at pH 4. Extraction was carried out with multi-metal solution with $[Ca]_0 = 3$ mmol/L, $[Mn]_0 = 300$ mmol/L, $[Mg]_0$, and $[Na]_0 = 100$ mmol/L and $[SO_4^{2-}]_{tot} = 250$ mmol/L. Temperature was 25°C.

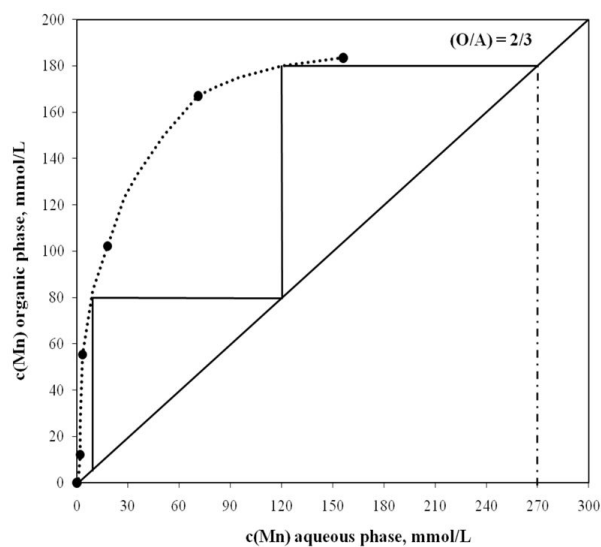


Figure 12. The effect of aqueous phase concentration on manganese extraction on 25 vol-% CYANEX 272 at pH 4.5. Extraction was carried out with multi-metal solution with $[Ca]_0 = 3$ mmol/L, $[Mn]_0 = 300$ mmol/L, $[Mg]_0$, and $[Na]_0 = 100$ mmol/L and $[SO_4^{2-}]_{tot} = 250$ mmol/L. Temperature was 25°C.

Extraction of manganese at low concentration (< 300 mmol/L) can be done with 25vol-% CYANEX 272 in two steps at pH 4.5, when phase ratio (O/A) is 2/3. If the feed concentration is higher, the phase ratio or reagent concentration should be increased. The result show that pH has a great affection on the extraction equilibrium of metals. The number of extraction steps needed at pH 4.0 is four times more than at 4.5. In the case, where Mn extraction has to be carried out at pH bellow 4, a stronger acid reagent is needed. Thio-phosphorus acid reagents are stronger than the oxygen analogues and could be good alternatives in such cases.

The production of high purity $MnSO_4$ solution was carried out by using 25 vol-% CYANEX 272 at $40^\circ C$ with an O/A phase ratio of 3/2 (Article II). About 99% of manganese was extracted in three steps with an increasing pH profile in the consecutive extraction stages. Scrubbing with 1 mmol/L H_2SO_4 solution effectively removed all co-extracted Mg and Ca from the organic phase. Stripping in two steps with H_2SO_4 solution at high O/A phase ratios (2 M in the first step and 1 M in the second) resulted in a pure $MnSO_4$ solution.

3.4 Octahedrally coordinated manganese oxide materials

The metal-adsorbing properties of OL-1, OMS-1, and OMS-2, which can be prepared using hydrometallurgical side-streams, were studied in heavy metal removal from multi-metal solutions in natural and hydrometallurgical environments (Articles III - VI). The studied and presented OMS materials are showin in Fig. 13. OMS-1 and OMS-2 were studied as non-supported for harmful metal ion uptake from natural conditions in Article IV. OL-1 and OMS-2 were synthesized via redox precipitation routes, whereas OMS-1 was synthesized by means of hydrothermal method by using OL-1 as the starting material. Regardless of the synthesis path, both materials had similar chemical properties. OMS-2 was not supported on silica and no column separation with that material was made.

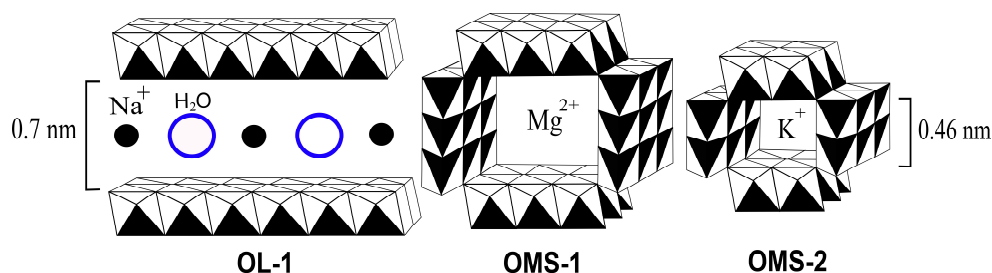


Figure 13. Tunnel structure with the template ions of OMS materials.

3.4.1 Synthesis and characterizing of OMS materials

The synthesized materials were identified by comparing the x-ray diffraction (XRD) profiles and IR spectra (Figs. 14 and 15) with literature data. The detailed peak pattern at $2\theta = 35 - 45^\circ$ is typical for monoclinic OL-1 (Drits et al., 1997) and so are the IR peaks at 425, 477 and 511 $1/cm$ (Al-Sagheer and Zaki, 2004). Little literature data are available for OMS-1, but the XRD and IR spectra measured in the present study agree with the literature values (Feng, 2004), (DeGuzman et al., 1994), (Tian et al., 1997). In particular, the peak at 750 $1/cm$ is characteristic for OMS-1 (Al-Sagheer, 2004), (Potter and Rossman, 1979). It is also noteworthy that no extra

peaks are found in the XRD profiles, indicating a complete conversion during the hydrothermal treatment. The measured XRD spectra and the found peaks at $2\theta = 12.8, 18.5, 28.9, 37.5, 42,$ and 50° confirm the form and purity of synthesized OMS-2 (Frias *et al.*, 2007). The selectivity of OMS-2 (K-cryptomelane) synthesis was interesting since the amount of magnesium (template for OMS-1 (Mg-todorokite) was over 1.5 times the amount of potassium in the initial synthesis mixture.

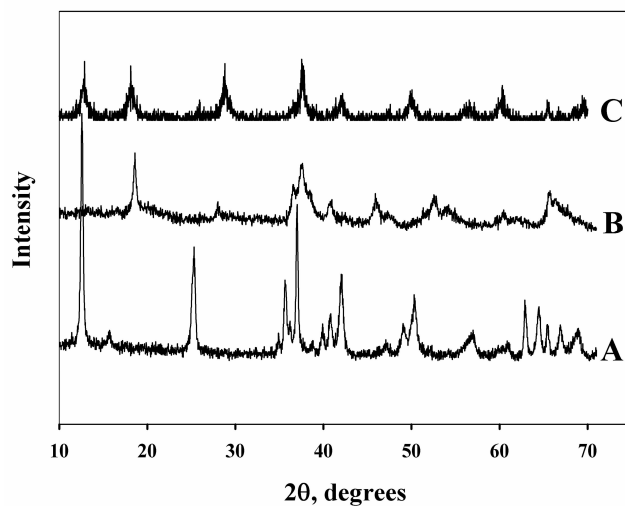


Figure 14. XRD patterns of Na-OL-1 (A), Mg-OMS-1 (B), and K-OMS-2 (C).

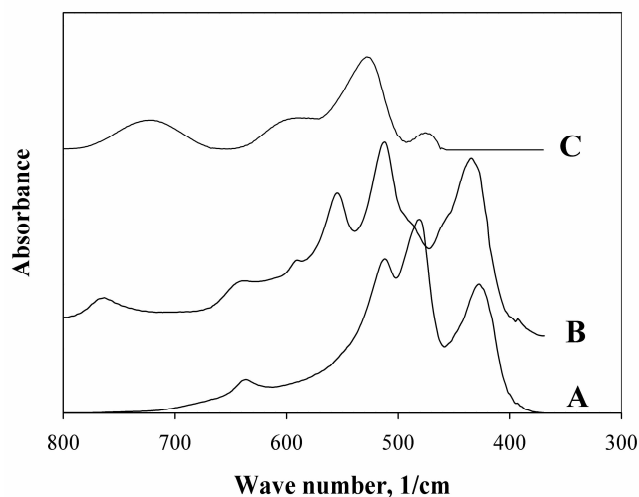
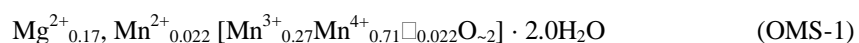


Figure 15. FTIR spectra of Na-OL-1 (A), Mg-OMS-1 (B), and K-OMS-2 (C).

The chemical composition of the synthesized materials was estimated from the results of elemental analysis, thermal analysis and determination of the average manganese oxidation state (AOS). The average oxidation states of Mn in the synthesized materials were 3.7 for OL-1, 3.8 for OMS-1 and 3.9 for OMS-2. It was assumed that the manganese exists as Mn^{2+} , Mn^{3+} and Mn^{4+} , structure of the materials after synthesis and gentle drying can be represented by the molecular formulas shown below. The bracketed species refer to the oxide framework, while other ions are exchangeable. Equilibrium and kinetic data, were also needed to determine the relative amounts of Mn^{2+} and Mn^{3+} in OMS materials.



3.4.2 Ion exchange properties

The acid-base properties and the effect of solution pH on equilibrium metal binding on OL-1, OMS-1, and OMS-2 were studied in Articles III - VI and the estimated parameter values are given in Table 6.

According to Articles III-VI, the studied materials behave as weak acids and metal uptake is possible with a reasonable capacity at pH values above 3. Consequently, batch uptake measurements at pH 5 were used here in order to get information on competitive sorption of metals and also on uptake rates. The metal concentrations of the model systems were chosen in such way that the amounts of potentially interfering ions were similar as in natural systems. The ion-exchange capacities of OMS materials and the pH dependence of metal uptake were elucidated by titration. The experimental and calculated acid titration curves are shown in Articles IV and VI. The number of ion-exchange sites was estimated by curve fitting and the values of 1.9, 2.3 and 2.2 mequiv/g were obtained for OL-1, OMS-1 and OMS-2, respectively. These values are substantially lower than the analyzed amounts of exchangeable cations, which were 3.5, 3.0, and 5.2 mequiv/g for Na-OL-1, Mg-OMS-1, and K-OMS-2, respectively.

Titration shows that acid uptake takes place by displacement of the metal counter-ions and a small contribution of Mn^{3+} dissolution is also present. The rate constant, k_{dis} , in Eq. (24) was estimated as $5.0 \cdot 10^{-2}$, $2.0 \cdot 10^{-3}$ and $5.0 \cdot 10^{-2}$ mol/(Ls) for OL-1, OMS-1 and OMS-2, respectively. The overall exchange rate is largely determined by desorption of the metal cations and no reliable estimate for the proton diffusion coefficient was obtained. The slower rate of OMS-1 is thus mainly due to slower diffusion of divalent Mg^{2+} when compared with univalent Na^{+} in OL-1. In view of the complexity of the OMS materials, the simple model gives a reasonable description of the systems.

Metals recovery

The ion exchange of the system was monitored by NaOH consumption and changes of the original counter-ions (Mg^{2+} , K^+ and Mn^{2+}) during the pre-equilibration step and further exchange (Fig. 16). Mg and K analysis showed that only about half of Mg^{2+} (in OMS-1) and K^+ (in OMS-2) present initially in the OMS structure were displaced in the ion exchange reaction with transition metal cations (Articles IV and VI). This indicates that the second half of the template ions inserted in synthesis is not exchangeable (possibly due to the steric block).

The Cu capacities of materials were 1.2 for OL-1 and 0.4 mmol/g for OMS-1 and OMS-2, when the initial Cu concentrations were 2 mmol/L. If the initial concentration was increased to 10 mmol/L the Cu capacities of OL-1, OMS-1 and OMS-2 were 1.8, 1.3 and 0.9 mmol/g, respectively. Moreover, the shape of the uptake curves suggests that in addition to normal ion exchange, there is another slower mechanism, which becomes important at higher solution concentrations. This was also found by (Eren, 2009) with MnO_2 materials and the explanation was two different sites with different adsorption energies and affinities. The presence of Ca with OMS-1 and OMS-2 had no significant affection of Cu loading (Article IV). The parameters estimated for Ni and Cd from the titration, kinetic and breakthrough data suggest strong steric exclusion from the tunnel sites. It seems, however, that the selectivity of OMS-2 for Ni over Ca and Mg can be sufficient in for example radio nuclide capture in natural system, where the metal concentrations are usually very low (Dyer *et al.*, 2000). When compared with the values measured by (Balakhonov *et al.*, 2008) for Pb and Ba, the Cu uptake capacity measured in this study for OMS-1 was about the same. Moreover, the copper capacities of OMS materials are quite similar to the copper uptake of conventional chelating ion exchangers. According to the results in our laboratory, iminodiacetic acid (IDA) bound on silica or polymer supports binds 0.5 - 1 mmol Cu/g. The studied materials and IDA resins prefer copper over nickel and cadmium.

The precipitation limit for copper was found to be about 20 mmol/L for the conditions of the experiments. Copper uptake was also determined both by solution analysis and by dissolving and analyzing the equilibrated solids. As shown in Article VI, both methods gave identical values within the analytical accuracy.

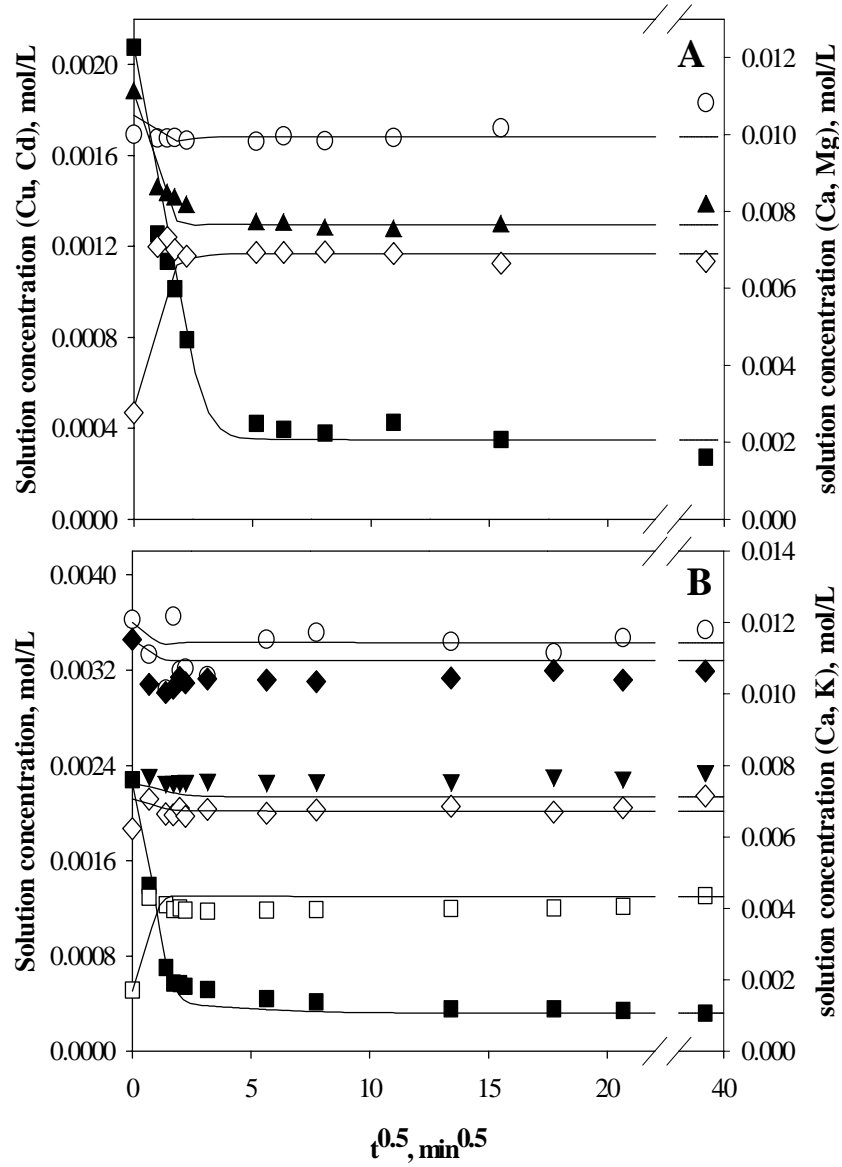


Figure 16. Uptake kinetics of metals on OMS-1 (A) and OMS-2 (B). $T = 25^{\circ}\text{C}$, $I = 0.1 \text{ M}$ (NaNO_3). Initial concentration of each metal was 2 mM , $c_{\text{Ca}}^{\text{init}} = 10 \text{ mM}$. Symbols: Cu (\blacksquare), Ni (\blacktriangledown), Cd (\blacktriangle), Ca (\circ), Mg (\diamond), K (\square), and Li (\blacklozenge). Solid lines were calculated from Eqs. (21 - 24) with the parameter values of Tables 6 and 7.

Table 6. Equilibrium binding parameters of OL-1, OMS-1 and OMS-2. $T = 25^{\circ}\text{C}$.

	OL-1 $p = 0.2$ $K_{\text{dis}} = 1.0$ $\nu_{\text{H}} = 0.5$		OMS-1 $p = 0.2$ $K_{\text{dis}} = 3.0$ $\nu_{\text{H}} = 0.8$		OMS-2 $p = 0.2$ $K_{\text{dis}} = 1.0$ $\nu_{\text{H}} = 1.1$	
Ion	$\log \kappa$ (κ in L/mol)	h (-)	$\log \kappa$ (κ in L/mol)	h (-)	$\log \kappa$ (κ in L/mol)	h (-)
H^+	7.5	1.0	8.0	1.0	8.0	1.0
Na^+	1	1.0	1.0	1.0	1.0	1.0
Li^+	n.d	n.d	nd.	nd.	9.0	0.1
K^+	n.d	n.d	nd.	nd.	12	0.4
Mg^{2+}	n.d	n.d	5.0	0.5	0.7	0.02
Mn^{2+}	3.3	0.5	7.0	0.5	7.0	0.5
Cu^{2+}	9.6	0.55	36.7	0.15	28	0.21
Ni^{2+}	40.7	0.07	3.7	0.16	12	0.25
Cd^{2+}	8.7 ^a	0.4 ^a	12.5	0.4	nd.	nd.
Ca^{2+}	n.d	n.d	0	0.0	0	0.01

nd.: Not determined.

a: Values are estimated from break-through data

Table 7. Mass transport parameter b_m for different cations in OL-1, OMS-2 and OMS-1 at 25°C .

Cation	$b_m (10^{-3} \text{ l/s})$		
	OL-1	OMS-1	OMS-2
H^+	40	4	4
Na^+	10	0.8	0.6
Li^+	n.d	nd.	0.6
K^+	n.d	nd.	0.8
Mg^{2+}	n.d	0.7	0.3
Mn^{2+}	2	0.3	0.3
Cu^{2+}	0.007	0.15	0.15
Ni^{2+}	0.004	nd.	0.1
Cd^{2+}	n.d	0.5	nd.
Ca^{2+}	n.d	0.6	0.7

nd.: Not determined.

The results show that both oxides have very high affinity for copper (κ values in Table 6). However, the binding capacity of OL-1 is clearly higher than that of OMS-1. The difference is much higher than expected from the ion-exchange capacities. It seems, therefore, that steric

exclusion from the narrower tunnel-system of OMS-1 should also be considered. The low uptake in OMS-1 can be correlated using a very small value for h_{Cu} in Eq. (21).

3.4.3 Metals separation with silica supported OMS-1 and OL-1

According to the characterization results shown in Articles V and VI, the MnO_2/SiO_2 composite has the optimum properties for column separation, when prepared by using colloidal silica (Ludox HS-40) at pH 5 and 110°C. A final heat-treatment at 250°C is needed to obtain sufficient physical strength. In a similar way, the nano-porous manganese oxides OL-1 and OMS-1 can be aggregated to sufficiently large particles with colloidal silica. Mechanical and chemical properties of OL-1-silica composite, however, were essentially worse than those of OMS-1-silica composite. As a consequence repeatable column separation experiments were done with silica supported OMS-1 material only.

The breakthrough curves of metal with silica supported OMS-1 are shown in Article VI. The results of the loading step show (Fig. 17A) that the metal uptake capacities of the prepared materials were quite small. The final copper loading was 0.14 mmol/g_{OMS}. This value is about half the uptake observed in equilibrium measurements at pH 5. The difference can be explained by considering the pH conditions in the bed. As shown in Article VI, pH in column front of metal pulse was about 3, which caused a competition between H^+ and Me^{2+} decreasing the metals uptake. The disproportionation reaction (Eq.22) becomes important at pH below 3 leading to slight material dissolution. It seems, therefore, that OMS-1 is too weakly acidic and the whole capacity cannot be effectively utilized in acid-form (Article VI). The balance between acid and metals uptake is satisfactorily explained by the model, as indicated by the relatively good agreement between the calculated and experimental curves.

According to the results, copper can be separated from Ni and Cd, but Mn dissolving from OMS-1 elutes very close to Cu (Fig. 17A). The selectivity coefficients $K_{Cu/Ni}$ and $K_{Cu/Cd}$ estimated from the breakthrough results were 21 and 3. The loaded metals were eluted from the bed with 0.05 M HNO_3 and the obtained outlet profiles are depicted in Fig. 17B. Metals desorbed relatively easily and the material was stable enough to endure several runs without marked dissolution. Comparison of the experimental and calculated curves indicates, however, that less copper was actually obtained than was expected on the basis of the loading curve. It seems possible that part of copper is bound at framework sites and desorption at the studied conditions can be very slow.

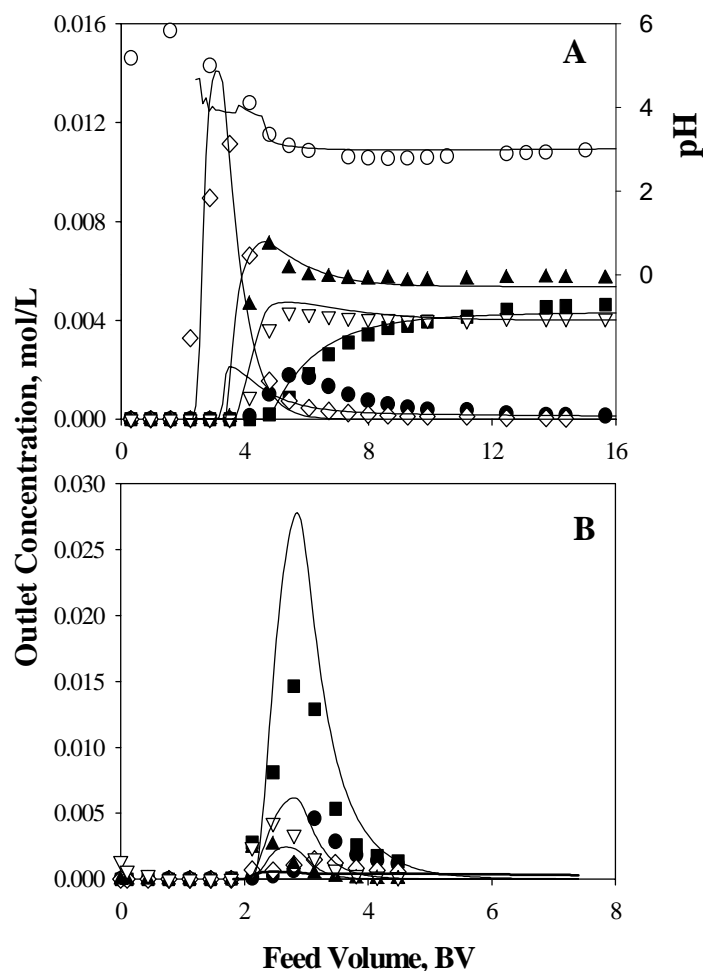


Figure 17. Outlet concentration profiles during the loading (A) and acid elution (B) steps in OMS-1/silica bed. $T = 25^{\circ}\text{C}$, $\text{BV} = 9.5 \text{ mL}$, feed flow rate 0.23 BV/min . Symbols: Mn (\bullet), Cu (\blacksquare), Ni (∇), Cd (\blacktriangle), Mg (\diamond), pH (\circ). Solid lines were calculated with the Eq.21-25.

A similar metal separation experiment was carried out also with silica-supported OL-1. The results shown in Article VI are qualitatively similar to Fig. 17 but they indicate that the metal capacities of OL-1/silica are even smaller than those of OMS-1/silica. The calculated breakthrough curves were obtained with an exchange capacity $0.4 \text{ mequiv/g}_{\text{OL}}$. It is possible that the low uptake rate of the transition metals in OL-1 (see Table 7) makes part of the material inaccessible during the fixed-bed experiment. Moreover, the large amount of eluted Mn could not be correlated with the proposed model.

4 CONCLUSIONS

Manganese and iron can be precipitated effectively from sulfate solution with several precipitant. Soda ash (Na_2CO_3) is one of the most favourable reagent for the recovery of Fe and Mn from sulfate media due to the relative low price, ease of control, formation of filterable solid, and favourable leaching properties. Also the gypsum formation is avoided by using soda ash. Oxidative precipitation with O_2 (air)/ SO_2 is economic, but the disadvantages are the need for very exact feed adjustment and the use of poisonous and corrosive SO_2 gas. Hydroxide and sulfide precipitations are widely used in hydrometallurgy, but the use in iron and manganese separation is challenging in terms of settling and filtration properties. In addition the leaching of metal sulfides and hydroxides need strong acid conditions (autoclave). The combined air oxidation and precipitation of Fe with limestone is advantageous in technical and economical viewpoints. The combination of limestone and air oxidation is a selective and effective method for removing iron from MnSO_4 solution. Also leaching of Mn as concentrated can be carried out with H_2SO_4 .

Temperature has a significant effect on the extraction selectivity of manganese and calcium with D2EHPA and CYANEX 272. Extraction Mn-Ca selectivity was found to increase with both reagents at low temperatures. The extraction order with D2EHPA, however, remains unchanged (Ca before Mn). The favourable extraction order of CYANEX 272 (Mn before Ca) and the operation of the SX above room temperature with lower solution viscosity and faster kinetics, are the advantages that make CYANEX 272 as the better choice for Mn extraction from Ca containing solution. The production of high purity MnSO_4 were carried out with 25 vol-% CYANEX 272 at 40°C with an O/A phase ratio of 3/2. About 99% of manganese was extracted in three steps with an increasing pH profile in the simulated back-flow extractions. Scrubbing with 1 mmol/L H_2SO_4 solution effectively removed all co-extracted Mg and Ca from the organic phase. Stripping in two steps with H_2SO_4 solution at high O/A phase ratios (2 M in the first step and 1 M in the second) resulted in a pure MnSO_4 solution. The pure MnSO_4 solution produced meets the requirements for a starting material for metallic manganese, manganese oxides or different manganese chemicals as well.

Three types of OMS manganese oxides, layered OL-1, tunnel-type OMS-1 and OMS-2, were synthesized, which the two former types were also supported on silica. The materials were tested for equilibrium metal uptake, uptake kinetics and for behavior in fixed-bed operations. The results showed the characteristic properties of the octahedral manganese oxides. The experimental data were correlated using the NICA equilibrium model and the Nernst-Planck equation for ion transport in the solids.

The results of equilibrium and kinetic experiments indicate that both oxides have high affinity for transition metals Cu, Ni and Cd, and reasonable exchange rates can be attained because of the small particle dimensions. These properties can be utilized in cyclical fixed-bed operation, when the OMS micro-crystals are supported on porous silica. The breakthrough behavior correlates relatively well with the proposed model and thus, allowing simulation at different conditions. Some drawbacks inherent to these materials must, however, be taken into account. The exchange capacity of OL-1 and OMS-1 cannot be fully utilized in a simple loading-acid elution cycle, because the materials are too weakly acidic. Moreover, instability at acidic conditions and in the presence of reducing agents limits their use in hydrometallurgical separations. For these reasons, more potential applications for OMS manganese oxides may be

found in hydrometallurgical tailings management, in environmental engineering, and in removal of radio-nuclides.

The results show that the studied OMS materials are promising for certain environmental applications, where harmful metal ions should be removed e.g. from mine effluents. However, the material must be transformed from the finely divided powder to a practically useful form. Excluding the smaller uptake capacities, the aggregation of OL-1 and OMS crystals with colloidal silica does not affect significantly their ion exchange properties.

REFERENCES

- Abbas, H., Askar, M.A., Abd-Elaziz, E.M. (1999). Recycling of zinc-carbon spent batteries: I. Production of manganese and zinc as sulfates. *Egyptian J. Chem.* , 42 (4), 361-373.
- Acharya, B.C., Nayak, B.K. (1998). Mineral chemistry of manganese ores associated with Precambrian Eastern Ghats complex of Andhra Pradesh-Orissa, India. (214-231, Ed.) *J. Miner. Petr. Ecol. Geol.* , 93.
- Acharya, C., Kar, R.N., Sukla, L.B. (2003). Studies on reaction mechanism of bioleaching of manganese ore. *Miner. Eng.* , 16, 1027-1030.
- Al-Sagheer, F. Z. (2004). Synthesis and surface characterization of OMS-1-type microporous manganese oxides: Implications for shape-selective oxidation catalysts. *Micropor. Mesopor. Mater.* , 67, 43-52.
- Al-Sagheer, F.A., Zaki, M.I. (2004). Synthesis and surface characterization of OMS-1-type microporous manganese oxides: Implications for shape-selective oxidation catalysts. *Micropor. Mesopor. Mater.* , 67, 43-52.
- Anonym. (2009). *Annual Review*. International Manganese Institute, IMnI.
- Arcos, D., Grandia, F., Domènech, C., Fernández, A.M., Villar, M.V., Muurinen, A., Carlsson, T., Sellin, P., Hernán, P. (2008). Long-term geochemical evolution of the near field repository: Insights from reactive transport modelling and experimental evidences. *Chem. Mater.* , 12, 3798-3804.
- Balakhonov, S.V., Churagulov, B.R., Gudilin, E.A. (2008). Selective cleaning of ions of heavy metals from water solutions using the H-form of todorokite synthesized by the hydrothermal method. *J. Surface Investigation, X-ray, Synchrotron Neutron Techniq.* , 2 (1), 152-155.
- Biswas, R.K., Singha, H.P. (2007). Densities, viscosities and excess properties of bis-2,4,4-trimethylpentylphosphinic acid (CYANEX 272)+diluent binary mixtures at 298.15 K and atmospheric pressure. *J. Mol. Liq.* , 135, 179-187.
- Brierley, J. (2008). A perspective on developments in biohydrometallurgy. *Hydrometallurgy* , 94, 2-7.
- Brierley, J.A., Brierley, C.L. (2001). Present and future commercial applications of biohydrometallurgy. *Hydrometallurgy* , 59, 233-239.
- Burgess, J. (1978). *Metal Ions in Solution*. London: John Wiley & Sons.
- Cameron, R.A., Lastra, R., Mortazavi, S., Gould, W.D., Thibault, Y., Bedard, P.L., Morin, L., Kennedy, K.J. (2009). Elevated-pH bioleaching of a low-grade ultramafic nickel sulfide ore in stirred-tank reactors at 5 to 45 °C. *Hydrometallurgy* , 99, 77-83.
- Carta, G., Lewus R.K. (1999). Film Model approximation for particle-diffusion-controlled multicomponent ion exchange. *Separ. Sci. Technol.* , 34, 2685-2697.
- Cheng, C. (2000). Purification of synthetic laterite leach solution by solvent extraction using D2EHPA. *Hydrometallurgy* , 56, 369-386.
- Claassen, J.O., Meyer, E.H.O., Rennie, J., Sandenbergh, R.F. (2002). Iron precipitation from zinc-rich solutions: defining the Zincor Process. *Hydrometallurgy* , 67, 87-108.

- Das, S.C., Sahoo, P.K., Rao, P.K. (1982). Extraction of manganese from low-grade manganese ores by FeSO₄ leaching. *Hydrometallurgy* , 8, 35-47.
- de Souza, C.C.B.M., Tenório, J.A.S. (2004). Simultaneous recovery of zinc and manganese dioxide from household alkaline batteries through hydrometallurgical processing. *J. Power Sources* , 136, 191-196.
- Dean, J. (1999). *Lange's handbook of chemistry* (15 ed.). New York: McGraw-Hill, Inc.
- DeGuzman, R.N., Shen, Y-F., Neth, E.J., Suib, S.L., O'Young, C-L., Levine, S., Newsam, J.M. (1994). Synthesis and characterization of octahedral molecular sieves (OMS-2) having the hollandite structure. *Chem. Mater.* , 6, 815-821.
- Devi, N.B., Nathsarma, K.C., Chakravorty, V. (2000). Separation of divalent manganese and cobalt ions from sulfate solutions using sodium salts of D2EHPA, PC 88A and CYANEX 272. *Hydrometallurgy* , 54, 117-131.
- Drits, V.A., Silvester, E., Gorshkov, A.I., Manceau, A. (1997). Structure of synthetic monoclinic Na-rich OL-1 and hexagonal OL-1: I. results from X-ray diffraction and selected-area electron diffraction. *Amer. Mineral.* , 82, 946-961.
- Dyer, A., Pillinger, M., Newton, J., Harjula, R., Möller, T., Amin, S., (2000). Sorption Behavior of Radionuclides on Crystalline Synthetic Tunnel Manganese Oxides. *Chem. Mater.* , 12, 3798-3804.
- El Absy, M. E. (1993). Separation of uranium from thorium on cryptomelane-type hydrous manganese dioxide. (145-153, Ed.) *J. Radioanal. Nuc. Chem.* , 172 (1).
- Elsherif, A. (2000). A study of the electroleaching of manganese ore. *Hydrometallurgy* , 55, 311-326.
- Elvers, B., Hawkings, S., Schulz, G. (1990). *Ullmann's Encyclopedia of Industrial Chemistry* (5 ed., Vol. A16). Weinheim.
- Eren, E. A. (2009). Removal of lead ions by acid activated and manganese oxide-coated bentonite. *J. Hazard. Mat.* , 161, 677-685.
- Feather, A., Sole, K.C., Dreisinger, D.B. (2000). Pilot-plant evaluation of manganese removal and cobalt purification by solvent extraction. Solvent Extraction for the 21st Century. Proceedings of ISEC '99. *Society of Chemical Industry (SCI)* , 1443-1448.
- Feng, Q., Kanoh, H., Ooi, K. (1999). Manganese oxide porous crystals. *J. Mater. Chem.* , 9, 319-333.
- Feng, X. T. (2004). Synthesis of todorokite at atmospheric pressure. *Chem. Mater.* , 16, 4330-4336.
- Frías, C., Díaz, G., Ocaña, N., Lozano, J.I. (2002). Silver, gold and lead recovery from bioleaching residues using the PLINT process. *Miner. Eng.* , 15, 877-878.
- Frías, S., Noursir, I., Barrio, M., Montes, T., López, M.A., Odriozola, J.A. (2007). Synthesis and characterization of cryptomelane- and birnessite-type oxides: precursor effect. *Mater. Character.* , 58, 776-781.
- Grace Davison. (n.d.). Product information from Grace Davison, Certified Quality System DIN ISO 9001 DQS Reg. No. 0924.
- Greenwood, N. E. (1984). *Chemistry of the Elements*. Oxford: Pergamon Press Ltd.

- Habashi, F. (2005). A short history of hydrometallurgy. *79*, 15-22.
- Habashi, F. (1999). *Textbook of Hydrometallurgy*. Québec: Métallurgie Extractive Québec.
- Halinen, A-K., Rahunen, N., Kaksonen, A.H., Puhakka, J.A. (2009). Heap bioleaching of a complex sulfide ore Part I: Effect of pH on metal extraction and microbial composition in pH controlled columns. *Hydrometallurgy* , *98*, 92-100.
- Havlik, T., Laubertova, M., Miskufova, A., Kondas, J., Vranka, F. (2005). Extraction of copper, zinc, nickel and cobalt in acid oxidative leaching of chalcopyrite at the presence of deep-sea manganese nodules as oxidant. *Hydrometallurgy* , *77*, 52-59.
- Ismael, M.R.C., Carvalho, J.M.R. (2003). Iron recovery from sulfate leach liquors in zinc hydrometallurgy. *Miner. Eng.* , *16*, 31-39.
- Jan, Y.-L. T.-C.-N. (2007). Associating characterization of bentonite-based buffer/backfill materials by distribution ratio (Rd) and (plastic index (PI). *J. Marine Sci. Technol.* , *15* (1), 17-23.
- Johnson, D. (2003). *The Economics of Manganese*. London: Roskill Information Services Ltd.
- Kholmogorov, A.G., Zhyzhaev, A.M., Kononov, U.S., Moiseeva, G.A., Pashkov, G.L. (2000). The production of manganese dioxide from manganese ores of some deposits of the Siberian region of Russia. *Hydrometallurgy* , *56*, 1-11.
- Kim, T-H., Senanayake, G., Kang, J-G., Sohn, J-S., Rhee, K-I., Lee, S-W., Shin, S-M. (2009). Reductive acid leaching of spent zinc-carbon batteries and oxidative precipitation of Mn-Zn ferrite nanoparticles. *Hydrometallurgy* , *96*, 154-158.
- Kinniburgh, D.G., van Riemsdijk, H., Koopal, L.K., Borkovec, M., Benedetti , M.F. and Avena, M.J. (1999). Ion binding to natural organic matter: competition, heterogeneity, stoichiometry and thermodynamic consistency. *Colloids Surfaces , A* *151*, 147-166.
- Koekemoer, L. (2005). Determination of viscosity and density of Di-(2-ethylhexyl) phosphoric acid + aliphatic kerosene. *J. Chem. Eng. Data* , *50*, 587-590.
- Kohga, T., Imamura, M., Takahashi, J., Tanaka, N., Nishizawa, T. (1995). Recovering iron, manganese, copper, cobalt, and high-purity nickel from sea nodules. *J. Miner. Met. Mater. Society* , *47* (12), 40-43.
- Kroschwitz, J.I., Howe-Grant, M. (1982). *Kirk-Othmer Encyclopedia of Chemical Technology* (4 ed., Vol. 15). New York: John Wiley & Sons.
- Le, L., Tang, J., Ryan, D., Valix, M. (2006). Bioleaching nickel laterite ores using multi-metal tolerant *Aspergillus foetidus* organism. *Miner. Eng.* , *19*, 1259-1265.
- Lee, E.Y., Noh, S-R., Cho, K-S., Ryu, H.W. (2001). Leaching of Mn, Co, and Ni from Manganese Nodules Using an Anaerobic Bioleaching Method. *J. Biosci. and Bioeng.* , *92* (4), 354-359.
- Leeuwen, H. (2008). Eigen Kinetics in Surface Complexation of Aqueous Metal Ions. *Langmuir* , *24*, 11718-11721.
- Loan, M., Newman, O.M.G., Cooper, R.M.G., Farrow, J.B., Parkinson, G.M. (2006). Defining the Paragoethite process for iron removal in zinc hydrometallurgy. *Hydrometallurgy* , *81*, 104-129.

- Lu, H., Zou, X. (2001). A comprehensive utilization process for black manganese-silver ores by pyrite reducing method. *Rare Metals (China)* , 20 (3), 142-146.
- Lu, Z.Y., Jeffery, M.I., Lawson, F. (2000). The effect of chloride ions on the dissolution of chalcopyrite in acidic solutions. *Hydrometallurgy* , 56, 189-202.
- Martell, A.E., Hancock, R.D. (1996). *Metal complexes in aqueous solutions*. New York: Plenum Press.
- Monhemius, A. (1977). Precipitation diagrams for metal hydroxides, sulfides, arsenates and phosphates. *Trans. Inst. Min. Met. , C* 86, 202-206.
- Morin, D., Lips, A., Pinches, T., Huisman, J., Frias, C., Norberg, A., Forssberg, E. (2006). BioMinE — integrated project for the development of biotechnology for metal bearing materials in Europe. *Hydrometallurgy* , 83, 69-76.
- Nan, J., Han, D., Cui, M., Yang, M., Pan, L. (2006). Recycling spent zinc manganese dioxide batteries through synthesizing Zn–Mn ferrite magnetic materials. *J. Hazard. Mater. , b133*, 257-261.
- Ndlovu, B., Mahlangu, T. (2008). Calcium and magnesium rejection from sulfate solutions in lateritic nickel solvent extraction using Versatic 10 acid-LIX 84-IC system. *J. Southern African Inst. Min. Met. , 108*, 223-228.
- Nijjer, S. (2000). *Deposition and Reduction of Manganese Dioxide on Alternative Anode Materials in Zinc Electrowinning*. D.Sc. dissertation, Norwegian University of Science and Technology.
- Pakarinen, J. (2006). Production of Manganese by Electrolysis. *Thermodynamic and kinetic phenomena in hydrometallurgical processes*. Espoo: TKK.
- Pakarinen, J., Paatero, E. (2007). Recovery of Manganese from Mixed Metal Solutions by Solvent Extraction with Organophosphorus Acid Extractants. *Topical Issues of Subsoil Usages*. St.Petersburg.
- Pitzer, K. (1991). *Activity Coefficients in Electrolyte Solutions* (2 ed.). Boston: CRC Press.
- Potter, R.M., Rossman, G.R. (1979). The tetravalent manganese oxides: identification, hydration, and structural relationships by infrared spectroscopy. *Amer. Mineral. , 64*, 1199-1218.
- Preston, J. (1994). The selective solvent extraction of cadmium by mixtures of carboxylic acids and trialkylphosphine sulfides. Part I. The origin and scope of the synergistic effect. *Hydrometallurgy* , 36, 61-78.
- Preston, J.S., du Preez, A.C. (1999). Solvent extraction of calcium and some divalent transition metals by mixtures of organophosphorus acids and bifunctional phosphonates. Solvent Extraction for the 21st Century. Proceedings of ISEC '99. *International Solvent Extraction Conference, ISEC'99* (pp. 305-309). London: Society of Chemical Inc.
- Puhakka, J., Kaksonen, A., Riekkola-Vanhanen, M. (2007). Heap Leaching of Black Schist. *Biomining* , 139-151.
- Ravitz, S.F., Wyman, W.F., Back, A.E., Tame, K.E. (1946). The dithionate process for recovery of manganese from low-grade ores. *Am. Ins. Min. Met. Eng. Met. Tech. , 13* (6), 10.
- Rawlings, D. (2002). Heavy metal mining using microbes. Annual Review. *Microbiology* , 56, 65-91.
- Ringbom, A. (1963). *Complexation in Analytical Chemistry*. New York: Wiley-Interscience.

- Ritcey, G. (2006). *Solvent extraction, principles and application to process metallurgy* (2 ed., Vol. 2). Ottawa: G.M. Ritcey & Associates incorporation.
- Ritcey, G.M. (2006). *Solvent extraction, principles and application to process metallurgy* (2 ed., Vol. 1). Ottawa: G.M. Ritcey & Associates incorporation.
- Runping, H., Weihua, Z., Wang, Y., Zhu, L. (2007). Removal of uranium(VI) from aqueous solutions by manganese oxide coated zeolite: discussion of adsorption isotherms and pH effect. *J. Environm. Radioact.* , 93, 127-143.
- Sayilgan, E., Kukrer, T., Civelekoglu, G., Ferella, F., Akcil, A., Veglio, F., Kitis, M. (2009). A review of technologies for the recovery of metals from spent alkaline and zinc-carbon batteries. *Hydrometallurgy* , 97, 158-166.
- Sayilgan, E., Kukrer, T., Yigit, N.O., Civelekoglu, G., Kitis, M. (2010). Acidic leaching and precipitation of zinc and manganese from spent battery powders using various reductants in ammoniacal and sulfuric acid solutions. *J. Hazard. Mater.* , 173, 137-143.
- Senanayake, G. (2004). A mixed surface reaction kinetic model for the reductive leaching of manganese dioxide with acidic sulfur dioxide. *Hydrometallurgy* , 73, 215-224.
- Senanayake, G., Das, G.K. (2004). A comparative study of leaching kinetics of limonitic laterite and synthetic iron oxides in sulfuric acid containing sulfur dioxide. *Hydrometallurgy* , 72, 59-72.
- Senanayake, G., Shin, S-M., Senaputra, A., Winn, A., Pugaev, D., Avraamides, J., Sohn Kim, D-J. (2010). Comparative leaching of spent zinc-manganese-carbon batteries using sulfur dioxide. *Hydrometallurgy* , 105, 36-41.
- Shan, X., Qin, W., Zhou, Z., Dai, Y. (2008). Prediction of pKa values of extractant using novel quantitative structure-property relationship models. *J. Chem. Eng. Data* , 53, 331-334.
- Sirola, K., Laatikainen, M., Lahtinen, M. Paatero, E. (2008). Separation of Copper and Nickel from Concentrated ZnSO₄ Solutions with Silica-Supported Chelating Adsorbents. *Sep. Purif. Technol.* , 64, 88-100.
- Snoeyink, V.L., Jenkins, D. (1980). *Water Chemistry*. New York: John Wiley & Sons.
- Söhnel, O., Garside, J. (1992). *Precipitation: basic principles and industrial applications*. Oxford: Butterworth-Heinemann.
- Stott, M.B., Watling, H.R., Franzmann, P.D., Sutton, D. (2000). The role of iron-hydroxy precipitates in the passivation of chalcopyrite during bioleaching. *Miner. Eng.* , 13, 1117-1127.
- Swanson, R. (1977). Liquid ion exchange: Organic molecules for hydrometallurgy. In: Lucas, B.H., Ritcey, G.M., Smith, H.W. (Eds.), Proceedings of ISEC 1977, CIM Spec. *International Solvent Extraction Conference, ISEC'77. 21*, pp. 3-8. Montreal: Can. Inst. Min. & Metall.
- Thomas, G., Whalley, B.J.P. (1958). The leaching of manganese from pyrolusite ore by pyrite. *Can. J. Chem. Eng.* , 36, 37-43.
- Tian, Z.R., Yin, Y-G., Suib, S.L. (1997). Effects of Mg²⁺ ions on the formation of todorokite type manganese oxide octahedral molecular sieves. *Chem. Mater.* , 9, 1126-1133.

- Tsakiridis, P.E., Agatzini, S.L. (2004). Process for the recovery of cobalt and nickel in the presence of magnesium and calcium from sulfate solutions by Versatic 10 and CYANEX 272. *Miner. Eng.* , 17, 535-543.
- Vu, H., Jandova, J., Lisa, K., Vranka, F. (2005). Leaching of manganese deep ocean nodules in FeSO₄-H₂SO₄-H₂O solutions. *Hydrometallurgy* , 77, 147-153.
- Watling, H. (2008). The bioleaching of nickel-copper sulfides. *Hydrometallurgy* , 91 (1-4), 70-88.
- Watling, H.R. (2006). The bioleaching of sulfide minerals with emphasis on copper sulfides. A review. *Hydrometallurgy* , 84, 81-108.
- Wei, D., Osseo-Asare, K. (1996). Particulate pyrite formation by the Fe³⁺/HS⁻ reaction in aqueous solutions: effects of solution composition. *Colloids and Surfaces A: Physicochemical and Engineering Aspects* , 118, 51-61.
- Weiss, S. (1977). *Manganese the other uses*. Hertfordshire: Metal Bulletin Books Ltd.
- Xin, B., Zhang, D., Zhang, X., Xia, Y., Wu, F., Chen, S., Li, L. (2009). Bioleaching mechanism of Co and Li from spent lithium-ion battery by the mixed culture of acidophilic sulfur-oxidizing and iron-oxidizing bacteria. *Bioresource Tech.* , 100, 6163-6169.
- Yaozhong, L. (2004). Laboratory study: simultaneous leaching silverbearing low-grade manganese ore and sphalerite concentrate. *Miner. Eng.* , 17 (9-10), 1053-1056.
- Zhang, W., Cheng, C.Y. (2007). Manganese metallurgy review. Part I: Leaching of ores/secondary materials and recovery of electrolytic/chemical manganese dioxide. *Hydrometallurgy* , 89, 137-159.
- Zhang, W., Cheng, C.Y. (2007). Manganese metallurgy review. Part II: Manganese separation and recovery from solution. *Hydrometallurgy* , 89, 160-177.
- Zhang, W., Muir, D.M., Singh, P. (2000a). Iron(II) oxidation by SO₂/O₂ in acidic media part I. Kinetics and mechanism. *Hydrometallurgy* , 55, 229-245.
- Zhang, W., Muir, D.M., Singh, P. (2000b). Iron(II) oxidation by SO₂/O₂ in acidic media part II. Effect of copper. *Hydrometallurgy* , 58, 117-125.
- Zhang, W., Singh, P., Muir, D. (2002). Oxidative precipitation of manganese with SO₂/O₂ and separation from cobalt and nickel. *Hydrometallurgy* , 63, 127-135.